NMR Studies of Chiral Discrimination Relevant to the Liquid Chromatographic Enantioseparation by a Cellulose Phenylcarbamate Derivative

Eiji Yashima, Chiyo Yamamoto, and Yoshio Okamoto*

Contribution from the Department of Applied Chemistry, School of Engineering, Nagoya University, Chikusa-ku, Nagoya 464-01, Japan

Received January 5, 1996[⊗]

Abstract: Chromatographic enantioseparation of 1,1′-bi-2-naphthol (**2**) and its mono- and di-*O*-methylated derivatives (**3a**, **3b**), 2,2′-dihydroxy-6,6′-dimethylbiphenyl (**4**), and 10,10′-dihydroxy-9,9′-biphenanthryl (**5**) has been performed on cellulose tris(5-fluoro-2-methylphenylcarbamate) (**1**) as a chiral stationary phase for high-performance liquid chromatography (HPLC). The complete base-line separation of **2** and **4** was achieved with the elution order of enantiomers such that the (*R*)-isomers eluted first followed by the (*S*)-isomers. The resolution of **5** and the *O*-methylated **3** was difficult on **1**. The cellulose derivative **1** dissolved in chloroform also exhibited a chiral discrimination for **2** and **4** in ^{1}H and ^{13}C NMR spectroscopies as well as in HPLC. The hydroxy and some aromatic protons and carbon resonances of **2** and **4** were clearly separated into a pair of peaks due to enantiomers in the presence of **1**. The binding geometry and dynamics between **1** and the enantiomers of **2** were investigated on the basis of spin−lattice relaxation time, ^{1}H NMR titrations, and intermolecular NOEs in the presence of **1**. These NMR data are fully consistent with the chromatographic elution order. These results, combined with molecular modeling, reveal the chiral discrimination rationale.

Introduction

Since biosystems consist of optically active chiral polymers, such as proteins, nucleic acids, and polysaccharides, living organisms often show quite different physiological behaviors toward one of a pair of enantiomers, especially chiral drugs.[1] Therefore, detailed investigations of the pharmacokinetics, physiological, toxicological, and metabolic activities of both enantiomers of the chiral drugs have become essential for the development of chiral drugs in the pharmaceutical industry.[2,3] Moreover, optically active compounds have recently aroused wide interest in many fields dealing with natural products, agrochemicals, and ferroelectric liquid crystals; therefore, their preparation and analysis are of increasing importance.

Chromatographic enantioseparations, particularly resolution by high-performance liquid chromatography (HPLC), have considerably advanced during the past decade not only for determining their optical purity but also for obtaining optical isomers, and in the pharmaceutical industry, chiral HPLC has become essential for the research and development of chiral drugs.[2,3] The preparation of a chiral stationary phase (CSP) capable of effective chiral recognition is the key to this separation technique. Therefore, many CSPs for HPLC have been prepared, and about 110 CSPs have already been on the market.[3,4]

There are basically two types of CSPs. One consists of a chiral small molecule that is usually bound to a support silica gel, and the second is derived from a chiral polymer being used as a porous gel or with silica gel. A great number of former CSPs have been prepared, and the clarification of the chiral discrimination mechanism on the CSPs have been attempted using spectroscopic[5] and computational methods.[6] The CSPs that have been most intensively studied in this respect are cyclodextrin-based CSPs and Pirkle-type CSPs.[5,6] The rational models of interactions between the CSPs and enantiomers have been proposed on the basis of the structural data of a crystalline 1:1 complex of a chiral selector and an enantiomer by X-ray[7] and the solution NMR experiments including intermolecular

[⊗] Abstract published in *Advance ACS Abstracts,* April 15, 1996.

(1) (a) Waldeck, B. *Chirality* **1993**, *5*, 350−355. (b) Millership, J. S.; Fitzpatrick, A. *Chirality* **1993**, *5*, 573−576. (c) White, C. A. In *A Practical Approach to Chiral Separations by Liquid Chromatography;* Subramanian, G., Ed.; VCH: New York, 1994; Chapter 1. (d) Cardwell, J. *J. Chromatogr. A* **1995**, *694*, 39−48.

(2) Mutton, I. M. In *A Practical Approach to Chiral Separations by Liquid Chromatography;* Subramanian, G., Ed.; VCH: New York, 1994; Chapter 11.

(3) (a) Stinson, S. C. *Chem. Eng. News* **1994**, Sep 19, 38−72. (b) Stinson, S. C. *Chem. Eng. News* **1995**, Oct 9, 44−74.

(4) Reviews: (a) Allenmark, S. G. *Chromatographic Enantioseparation*; Ellis Horwood: Chichester, 1988. (b) *A Practical Approach to Chiral Separations by Liquid Chromatography*; Subramanian, G., Ed.; VCH: New York, 1994. (c) Armstrong, D. W. *Anal. Chem.* **1987**, *59*, 84−91A. (d) Okamoto, Y. *Chemtech* **1987**, 176−181. (e) Pirkle, W. H.; Pochapsky, T. C. *Chem. Rev.* **1989**, *89*, 347−362. (f) Taylor, D. R.; Maher, K. *J. Chromatogr. Sci.* **1992**, *30*, 67−85. (g) *Chiral Separations. Fundamental Aspects and Applications;* Lindner, W., Ed.; *J. Chromatogr. A* **1994**, 666.

(5) For NMR studies of chiral recognition with the aid of chromatography using optically active small molecule CSPs, see: (a) Feibush, B.; Figueroa, A.; Charles, R.; Onan, K. D.; Feibush, P.; Karger, B. L. *J. Am. Chem. Soc.* **1986**, *108*, 3310−3318. (b) Pirkle, W. H.; Pochapsky, T. C. *J. Am. Chem. Soc.* **1986**, *108*, 5627−5628. (c) Pirkle, W. H.; Pochapsky, T. C. *J. Am. Chem. Soc.* **1987**, *109*, 5975−5982. (d) Uccello-Barretta, G.; Rosini, C.; Pini, D.; Salvadori, P. *J. Am. Chem. Soc.* **1990**, *112*, 2707−2710. (e) Lipkowitz, K. B.; Raghothama, S.; Yang, J. *J. Am. Chem. Soc.* **1992**, *114*, 1554−1562. (f) Lohmiller, K.; Bayer, E.; Koppenhoefer, B. *J. Chromatogr. A* **1993**, *634*, 65−77. (g) Oi, S.; Ono, H.; Tanaka, H.; Matsuzaka, Y.; Miyano, S. *J. Chromatogr. A* **1994**, *659*, 75−86. (h) Uccello-Barretta, G.; Pini, D.; Rosini, C.; Salvadori, P. *J. Chromatogr. A* **1994**, *666*, 541−548. (i) Pirkle, W. H.; Welch, C. J. *J. Chromatogr. A* **1994**, *683*, 347−353. (j) Pirkle, W. H.; Selness, S. R. *J. Org. Chem.* **1995**, *60*, 3252−3256. (k) Kuroda, Y.; Suzuki, Y.; He, J.; Kawabata, T.; Shibukawa, A.; Wada, H.; Fujima, H.; Go-oh, Y.; Imai, E.; Nakagawa, T, *J. Chem. Soc., Perkin Trans. 2* **1995**, 1749−1759.

(6) For reviews of computational studies of chiral recognition with the aid of chromatography using optically active small molecule CSPs, see: (a) Lipkowitz, K. B. In *A Practical Approach to Chiral Separations by Liquid Chromatography*; Subramanian, G., Ed.; VCH: New York, 1994; Chapter 2. (b) Lipkowitz, K. B.; Anderson, A. G. In *Computational Approaches in Supramolecular Chemistry;* Wipff, G., Ed.; Kluwer: Dordrecht, 1994; pp 183−198. (c) Lipkowitz, K. B. *J. Chromatogr. A* **1995**, *694*, 15−37. (d) Topiol, S.; Sabio, M.; Moroz, J.; Caldwell, W. B. *J. Am. Chem. Soc.* **1990**, *110*, 8367−8376.

S0002-7863(96)00050-9 CCC: $12.00

NOE studies[5] which have been proved to be very powerful tools for understanding the nature of chiral discrimination occurring in solution between small molecules as exemplified by host−guest complexation.[8]

The CSPs composed of chiral polymers such as polyacrylamides,[9] one-handed helical polymethacrylates,[10] polyamides,[11] proteins,[12] and polysaccharide derivatives[13,14] have also been extensively studied, many of which are now commercially available. In contrast to the small-molecule CSPs, very few mechanistic studies on chiral discrimination at a molecular level have been done particularly by spectroscopic methods on polymeric CSPs.[15] Chiral polymers usually have a number of different binding sites with a different affinity to enantiomers and the determination of their exact structures in both solid and solution is laborious. This makes it difficult to evaluate a precise chiral recognition mechanism. The only exception may be some special protein−ligand and DNA−drug complexes, whose structures have been determined by either X-ray or NMR analysis in solution.[16]

We have found that phenylcarbamate derivatives of cellulose and amylose show high resolving power as CSPs when coated on macroporous silica gel and can separate a wide range of racemates including many drugs.[14] Some of the derivatives have been commercialized and used as very popular CSPs.[17] However, the chiral recognition mechanism on the phenylcarbamate derivatives at a molecular level remains elusive, although a qualitative explanation has been given on the basis of chromatographic enantioseparation[14] and computational studies.[18]

An NMR spectroscopic study on the chiral recognition mechanism of polymer systems often fails because most polymers are soluble only in the solvents which prevent enantiomer discrimination. Most phenylcarbamate derivatives of the polysaccharides with high chiral resolving power as CSPs are typical cases. They are soluble only in polar solvents, such as tetrahydrofuran (THF), acetone, and pyridine. In such polar solvents, the phenylcarbamate derivatives show poor chiral recognition for enantiomers because the solvents preferentially interact with the polar carbamate residues which are the most important binding site for chiral discrimination.

However, we recently found that cellulose tris(4-(trimethylsilyl)phenylcarbamate) (CTSP)[19] is soluble in chloroform and shows chiral discrimination in ^{1}H NMR spectroscopy as well as in HPLC. For instance, the methine proton of *trans*-2,3-diphenyloxirane was split into two singlet resonances in the presence of CTSP,[19] indicating that CTSP can discriminate the enantiomers even in solution. The elution order of *trans*-2,3-diphenyloxirane on CTSP correlated well with the downfield shift of the (−)-isomer observed in the ^{1}H NMR. CTSP can work as the chiral shift reagent and discriminates the enantiomers of the Tröger base, benzoin, mandelic acid, and several *sec*-alcohols, such as 2-butanol and 2-octanol in $CDCl_3$.[20] However, the differences in the chemical shifts of the enantiomers in the presence of CTSP were too small to obtain reliable

(7) (a) Pirkle, W. H.; Burke, J. A., III; Wilson, S. R. *J. Am. Chem. Soc.* **1989**, *111*, 9222−9223. (b) Francotte, E.; Rihs, G. *Chirality* **1989**, *1*, 80−85.

(8) (a) Cram, D. J. *Angew. Chem., Int. Ed. Engl.* **1988**, *27*, 1009−1020. (b) Lehn, J. M. *Angew. Chem., Int. Ed. Engl.* **1988**, *27*, 89−112. (c) Dharanipragada, R.; Ferguson, S. B.; Diederich, F. *J. Am. Chem. Soc.* **1988**, *110*, 1679−1690. (d) Echavarren, A.; Galán, A.; Lehn, J. M.; Mendoza, de J. *J. Am. Chem. Soc.* **1989**, *111*, 4994−4995. (e) Spisni, A.; Corradini, R.; Marchelli, R.; Dossena, A. *J. Org. Chem.* **1989**, *54*, 684−688. (f) Sanderson, P. E. J.; Kilburn, J. D.; Still, W. C. *J. Am. Chem. Soc.* **1989**, *111*, 8314−8315. (g) Liu, R.; Sanderson, P. E. J.; Still, W. C. *J. Org. Chem.* **1990**, *55*, 5184−5186. (h) Rebek, J., Jr. *Angew. Chem., Int. Ed. Engl.* **1990**, *29*, 245−255. (i) Webb, T. H.; Suh, H.; Wilcox, C. S. *J. Am. Chem. Soc.* **1991**, *113*, 8554−8555. (j) Seel, C.; Vögtle, F. *Angew. Chem., Int. Ed. Engl.* **1992**, *31*, 528−549. (k) Coterón, J. M.; Vicent, C.; Bosso, C.; Penadés, S. *J. Am. Chem. Soc.* **1993**, *115*, 10066−10076. (l) Webb, T. H.; Wilcox, C. S. *Chem. Soc. Rev.* **1993**, 383−395. (m) Böhmer, V. *Angew. Chem., Int. Ed. Engl.* **1995**, 34, 713−745.

(9) (a) Blaschke, G. *Angew. Chem., Int. Ed. Engl.* **1980**, *19*, 13−24. (b) Blaschke, G. *J. Liq. Chromatogr.* **1986**, *9*, 341−368.

(10) (a) Yuki, H.; Okamoto, Y.; Okamoto, I. *J. Am. Chem. Soc.* **1980**, *102*, 6356−6358. (b) Okamoto, Y.; Okamoto, I.; Yuki, H.; Murata, S.; Noyori, R.; Takaya, H. *J. Am. Chem. Soc.* **1981**, *103*, 6971−6973. (c) Okamoto, Y.; Hatada, K. *J. Liq. Chromatogr.* **1986**, *9*, 369−384. (d) Okamoto, Y.; Yashima, E. *Prog. Polym. Sci.* **1990**, *15*, 263−298. (e) Chance, J. M.; Geiger, J. H.; Okamoto, Y.; Aburatani, R.; Mislow, K. *J. Am. Chem. Soc.* **1990**, *112*, 3540−3547. (f) Okamoto, Y.; Nakano, T. *Chem. Rev.* **1994**, *94*, 349−372.

(11) Saigo, K. *Prog. Polym. Sci.* **1992**, *17*, 35−86.

(12) For reviews, see ref 4a,b,g. (a) Hermansson, J.; Eriksson, M. *J. Liq. Chromatogr.* **1986**, *9*, 621−639. (b) Allenmark, S. G. *J. Liq. Chromatogr.* **1986**, *9*, 425−442. (c) Miwa, T.; Miyakawa, T. *J. Chromatogr.* **1987**, *408*, 316−322. (d) Erlandsson, P.; Marle, I.; Hansson, L.; Isaksson, R.; Pettersson, C.; Pettersson, G. *J. Am. Chem. Soc.* **1990**, *112*, 4573−4574. (e) Wainer, I. W.; Jadaud, P.; Schombaum, G. R.; Kadadker, S. V.; Henry, M. P. *Chromatographia* **1988**, *25*, 903−907. (f) Noctor, T.; Felix, G.; Wainer, I. W. *Chromatographia* **1991**, *31*, 55−59. (g) Haginaka, J.; Murashima, T.; Seyama, C. *J. Chromatogr. A* **1994**, *666*, 203−210.

(13) For cellulose esters as CSPs, see: (a) Hesse, G.; Hagel, R. *Chromatographia* **1973**, *6*, 277−280. (b) Becher, G.; Mannschreck, A. *Chem. Ber.* **1981**, *114*, 2365−2368. (c) Okamoto, Y.; Kawashima, M.; Yamamoto, K.; Hatada, K. *Chem. Lett.* **1984**, 739−742. (d) Ichida, A.; Shibata, T.; Okamoto, I.; Yuki, Y.; Namikoshi, H.; Toda, Y. *Chromatographia* **1984**, *19*, 280−284. (e) Francotte, E.; Wolf, R. M.; Lohmann, D. *J. Chromatogr.* **1985**, *347*, 25−37. (f) Okamoto, Y.; Aburatani, R.; Hatada, K. *J. Chromatogr.* **1987**, *389*, 95−102. (g) Wainer, I. W.; Stiffin, R. M.; Shibata, T. *J. Chromatogr.* **1987**, *139*, 139−151. (h) Francotte, E.; Wolf, R. M. *Chirality* **1990**, *2*, 16−31. (i) Francotte, E. *J. Chromatogr. A* **1994**, *666*, 565−601.

(14) For reviews of phenylcarbamates of polysaccharides as CSPs, see: (a) Shibata, T.; Okamoto, I.; Ishii, K. *J. Liq. Chromatogr.* **1986**, *9*, 313−340. (b) Okamoto, Y.; Aburatani, R.; Hatano, K.; Hatada, K. *J. Liq. Chromatogr.* **1988**, *11*, 2147−2163. (c) Okamoto, Y.; Kaida, Y. *J. High Resolut. Chromatogr.* **1990**, *13*, 708−712. (d) Okamoto, Y.; Kaida, Y.; Aburatani, R.; Hatada, K. In *Chiral Separations by Liquid Chromatography;* Ahuja, S., Ed.; ACS Symposium Series 471; American Chemical Society: Washington, DC, 1991; pp 101−113. (e) Okamoto, Y.; Kaida, Y. *J. Chromatogr. A* **1994**, *666*, 403−419. (f) Dingene, J. In *A Practical Approach to Chiral Separations by Liquid Chromatography*; Subramanian, G., Ed.; VCH: New York, 1994; Chapter 6. (g) Oguni, K.; Oda, H.; Ichida, A. *J. Chromatogr. A* **1995**, *694*, 91−100. (h) Yashima, E.; Okamoto, Y. *Bull. Chem. Soc. Jpn.* **1995**, *68*, 3289−3307. For other leading references, see: (i) Okamoto, Y.; Kawashima, M.; Hatada, K. *J. Am. Chem. Soc.* **1984**, *106*, 5357−5359. (j) Okamoto, Y.; Kawashima, M.; Hatada, K. *J. Chromatogr.* **1986**, 363, 173−186. (k) Okamoto, Y.; Aburatani, R.; Hatada, K. *Bull. Chem. Soc. Jpn.* **1990**, *63*, 955−957. (l) Okamoto, Y.; Ohashi, T.; Kaida, Y.; Yashima, E. *Chirality* **1993**, *5*, 616−621. (m) Ishikawa, A.; Shibata, T. *J. Liq. Chromatogr.* **1993**, *16*, 859−878. (n) Chankvetadze, B.; Yashima, E.; Okamoto, Y. *J. Chromatogr. A* **1994**, *670*, 39−49. (o) Yashima, E.; Fukaya, H.; Okamoto, Y. *J. Chromatogr. A* **1994**, *677*, 11−19. (p) Maeda, K; Okamoto, Y; Morlender, N; Eventova, I; Biali, S. E; Rappoport, Z. *J. Am. Chem. Soc.* **1995**, *117*, 9686−9689.

(15) For NMR studies of chiral recognition on polymeric CSPs, see: (a) Oguni, K.; Matsumoto, A.; Isokawa, A. *Polym. J.* **1994**, *26*, 1257−1261. (b) Pinkerton, T. C.; Howe, W. J.; Ulrich, E. L.; Comiskey, J. P.; Haginaka, J.; Murashima, T.; Walkenhorst, W. F.; Westler, W. M.; Markley, J. L. *Anal. Chem.* **1995**, *67*, 2354−2367. For computational studies of chiral recognition on polymeric CSPs, see: (c) Wolf, R. M.; Francotte, E.; Lohmann, D. *J. Chem. Soc., Perkin Trans. 2* **1988**, 893−901.

(16) For reviews: (a) Schulz, G. E.; Schirmer, R. H. *Principles of Protein Structure;* Springer-Verlag: New York, 1979; Chapter 10. (b) Saenger, W. *Principles of Nucleic Acid Structure;* Springer-Verlag: New York, 1984; Chapter 16. (c) Wüthrich, K. *NMR of Proteins and Nucleic Acids;* Wiley: New York, 1986; Chapter 15 and references cited therein. (d) Lee, M.; Shea, R. G.; Hartley, J. A.; Kissinger, K.; Pon, R. T.; Vesnaver, G.; Breslauer, K. J.; Dabrowiak, J. C.; Lown, J. W. *J. Am. Chem. Soc.* **1989**, *111*, 345−354. (e) Zhang, X.; Patel, D. J. *Biochemistry* **1990**, *29*, 9451−9466. (f) Eriksson, M.; Leijon, M.; Hiort, C.; Nordén, B.; Gräulund, A. *J. Am. Chem. Soc.* **1992**, *114*, 4933−4934. (g) Paloma, L. G.; Smith, J. A.; Chazin, W. J.; Nicolaou, K. C. *J. Am. Chem. Soc.* **1994**, *116*, 3697−3708. (h) Blaskó, A.; Browne, K. A.; Bruice, T. C. *J. Am. Chem. Soc.* **1994**, *116*, 3726−3737.

(17) Commercialized as CHIRALCEL and CHIRALPAK by Daicel Chemical Industries, Ltd., Tokyo, Japan.

(18) Yashima, E.; Yamada, M.; Kaida, Y.; Okamoto, Y. *J. Chromatogr. A* **1995**, *694*, 347−354.

(19) Yashima, E.; Yamada, M.; Okamoto, Y. *Chem. Lett.* **1994**, 579−582.

(20) Okamoto, Y.; Yashima, E. *Macromol. Symp.* **1995**, *99*, 15−23.

Chart 1

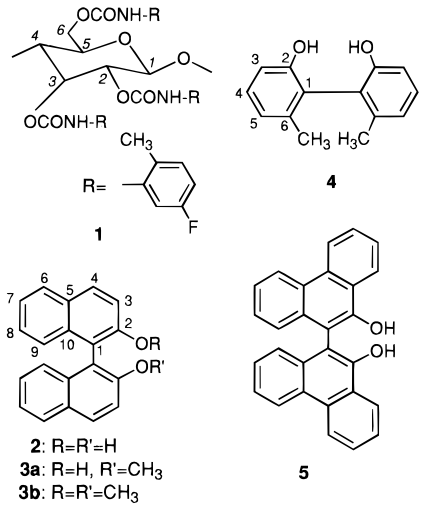

data on the chiral recognition rationale through ^{1}H NMR titrations and NOE measurements because of weak binding. Very recently, we have found that cellulose tris(5-fluoro-2-methylphenylcarbamate) (**1**) (Chart 1) is also soluble in chloroform[21] and is capable of discriminating enantiomers of 1,1′-bi-2-naphthol (**2**) and 2,2′-dihydroxy-6,6′-dimethylbiphenyl (**4**) in ^{1}H and ^{13}C NMR with large chemical shift changes of the enantiomers as well as in HPLC accompanying the large separation factors ($\alpha > 3$). These results suggest that the system consisting of **1** and **2** or **4** will be suitable for elucidating the chiral discrimination mechanism on cellulose-based CSPs at a molecular level through NMR studies.

Results and Discussion

Chromatographic Enantioseparation. Figure 1 shows a chromatogram of the resolution of racemic 1,1′-bi-2-naphthol (**2**) on a column packed with cellulose tris(5-fluoro-2-methylphenylcarbamate) (**1**). The peaks were detected by a UV detector and identified by a polarimetric detector. The *(R)*-(+)-**2** and *(S)*-(−)-**2** enantiomers eluted at retention times of t_1 and t_2, respectively, showing complete separation. Chromatographic parameters, capacity factors, $k_1' = (t_1 - t_0)/t_0$ and $k_2' = (t_2 - t_0)/t_0$, and separation factor ($\alpha = k_2'/k_1'$) were found to be 2.31, 9.77, and 4.23, respectively. The dead time t_0 was estimated by using 1,3,5-tri-*tert*-butylbenzene as a nonretained compound.[22] This indicates that *(S)*-(−)-**2** interacts more strongly with the stationary phase consisting of **1** than *(R)*-(+)-**2**.

To investigate the role of hydrogen bonding interaction between the CSP **1** and **2** in chiral recognition, one or both of the hydroxy groups of **2** were methylated (**3a** and **3b**). The chromatographic results of enantioseparation of **2** and four analogues (**3a**, **3b**, **4**, and **5**) on the same column **1** are given in Table 1. For **3a** and **3b**, a remarkable decrease of interaction in retention (k_1') and enantioselectivity (α) toward the CSP **1** was observed. These results indicate that hydrogen bonding interaction through the hydroxy groups of **2** is the main force for its retention and separation, and the simultaneous hydrogen bonding through the two hydroxy groups may be essential for effective resolution.

An analogous biaryl compound, 2,2′-dihydroxy-6,6′-dimethylbiphenyl (**4**), was also resolved completely with a large α value (3.22), and the (*S*)-isomer was more retained as well as in the resolution of **2**. On the other hand, 10,10′-dihydroxy-9,9′-biphenanthryl (**5**) was hardly separated under identical conditions. Bulky aromatic groups around the OH groups may disturb the efficient hydrogen bonding. From the separation factor (α), the difference in free energy ($\Delta\Delta G°$) at a given temperature can be calculated by using eq 1 (Table 1), where R

$$\Delta\Delta G° = -RT \ln \alpha \qquad (1)$$

is the gas constant of 1.987 cal mol^{-1} K^{-1} and T is the absolute temperature in K. These values can also be estimated by the NMR titration method in solution which will be discussed later.

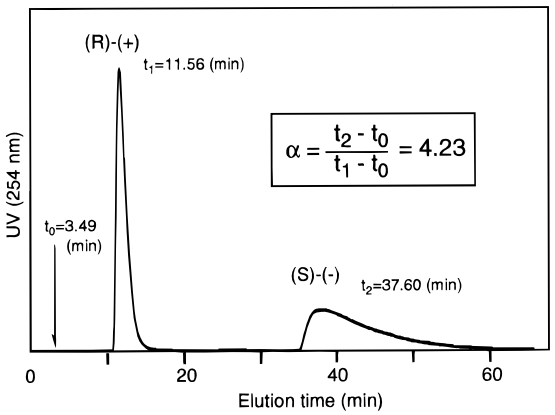

Figure 1. Chromatogram of the enantioseparation of (*RS*)-1,1′-bi-2-naphthol (**2**) on CSP **1** with hexane−2-propanol (90/10) as the eluent at 20 °C. Column, 25 × 0.46 cm i.d.; flow rate, 1.0 mL min^{-1}.

Table 1. Capacity Factor (k_1'), Separation Factor (α), and the Difference in Free Energy ($\Delta\Delta G$) in the Enantioseparation of **2**−**5** on the CSP **1** at 23 °C[a]

racemate	k_1' [b]	α	$\Delta\Delta G$[c] (kcal·mol^{-1})
2	2.31 ((*R*)-(+))	4.23	0.85
	0.85 ((*R*)-(+))[d]	3.22[d]	0.69[d]
3a[d]	0.73 ((*R*)-(+))	ca. 1	ca. 0
3b[d]	0.46	1.00	0
4	1.39 ((*R*)-(+))	3.22	0.69
5	1.31 (−)	ca. 1	ca. 0

[a] Hexane−2-propanol (90/10) was used as the eluent at a flow rate of 1.0 mL min^{-1}. [b] The sign in parentheses represents the absolute configuration and/or optical rotation of the first-eluting enantiomer. [c] $\Delta\Delta G$ can be estimated by using eq 1 (see text). [d] The eluent was hexane−2-propanol (70/30).

One-Dimensional NMR Studies. The phenylcarbamate **1** can resolve many enantiomers in addition to **2** and **4** as a CSP in HPLC.[21] Since **1** is soluble in chloroform, one can investigate the chiral discrimination of **1** in solution by ^{1}H and ^{13}C NMR spectroscopies.

Figure 2 shows the 500 MHz ^{1}H NMR spectra of (*RS*)-**2** in the absence (A) and presence (B) of **1** in $CDCl_3$. The peak assignments were done on the basis of 2D COSY and NOESY experiments. The assignments for **2** were identical to those in dimethyl sulfoxide-d_6.[23] Each of the hydroxy and naphthyl protons (H4 and H6) of the enantiomers of **2** were significantly separated into two peaks in the presence of **1**. Other naphthyl protons were also split with relatively small chemical shift differences (Table 2). This clearly indicates that **1** can recognize the enantiomers even in solution. The chemical shift differences ($\Delta\Delta\delta$) are sufficiently large enough to determine the ratio of the enantiomers, indicating that **1** can be used as a chiral shift

(21) Yashima, E.; Yamamoto, C.; Okamoto, Y. *Polym. J.* **1995**, *27*, 856−861.

(22) (a) Koller, H.; Rimböck, K.-H.; Mannschreck, A. *J. Chromatogr.* **1983**, *282*, 89−94. (b) Pirkle, W. H.; Welch, C. J. *J. Liq. Chromatogr.* **1991**, *14*, 1−8.

(23) Marin-Puga, G.; Horák, V.; Svoronos, P. *Collect. Czech. Chem. Commun.* **1993**, *58*, 77−81.

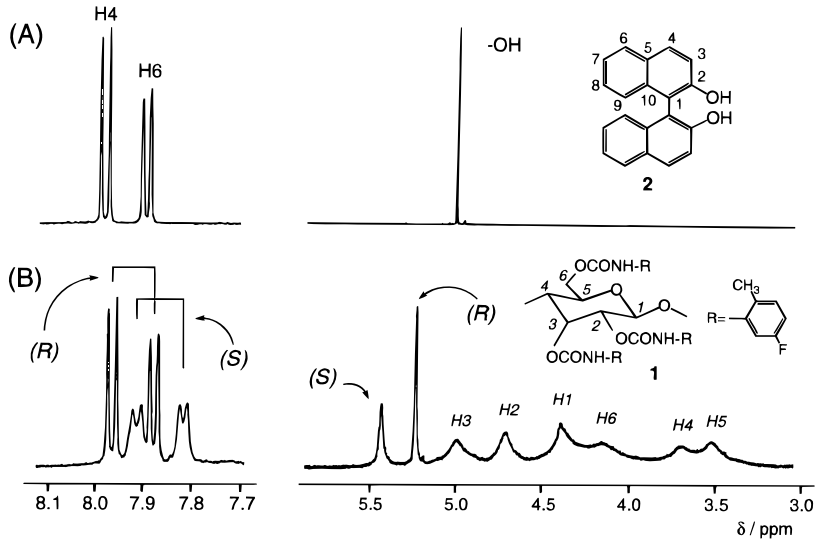

Figure 2. ^{1}H NMR spectra of selected region of (*RS*)-**2** (19.4 mM) in the absence (A) and presence (B) of **1** (36.1 mM glucose units) in $CDCl_3$ at 23 °C. The assignments were performed with 2D COSY and NOESY experiments.

Table 2. ^{1}H and ^{13}C NMR Chemical Shifts (ppm) of **2** in the Absence and the Presence of **1** in $CDCl_3$ at 23 °C

	^{1}H NMR				^{13}C NMR			
position	free[a]	**1**−(*S*)-**2**[b]	**1**−(*R*)-**2**[b]	ΔΔδ[c]	free[d]	**1**−(*S*)-**2**[e]	**1**−(*R*)-**2**[e]	ΔΔδ[c]
OH	5.036	5.435	5.234	0.201				
1					110.74	111.05	110.94	0.11
2					152.70	152.59	152.68	−0.09
3	7.391	7.358	7.385	−0.027	117.71	117.63	117.72	−0.09
4	7.985	7.917	7.967	−0.050	131.40	131.42	131.34	0.08
5					129.40	129.37	129.34	0.03
6	7.900	7.819	7.881	−0.062	128.38	128.31	128.36	−0.05
7	7.378	7.337	7.372	−0.035	124.02	123.94	123.97	−0.03
8	7.312	7.297	7.304	−0.007	127.47	127.42	127.40	0.02
9	7.156	7.137	7.145	−0.008	124.16	124.16	124.21	−0.05
10					133.35	133.52	133.41	0.11

[a] [(*RS*)-**2**] = 19.4 mM. [b] The chemical shifts of OH, H4, H6, and H9 proton resonances were based on the spectrum of (*RS*)-**2** (19.4 mM) in the presence of **1** (36.1 mM) (see Figure 2). Because of overlapping of the peaks, the other protons chemical shifts were measured separately for (*S*)- and (*R*)-**2** (each 9.7 mM) with **1** (18.1 mM). [c] Obtained by subtracting the **1**−(*R*)-**2** values from the **1**−(*S*)-**2** ones. [d] [(*RS*)-**2**] = 116 mM. [e] The chemical shifts of C1, C2, C3, C4, and C10 carbon resonances were based on the spectrum of (*RS*)-**2** (116 mM) in the presence of **1** (54.2 mM) (see Figure 3). Because of overlapping of the peaks, the other carbons chemical shifts were measured separately for (*S*)- and (*R*)-**2** (each 58.2 mM) with **1** (54.2 mM).

reagent. Although a large number of designed chiral hosts, chiral solvating agents, and chiral lanthanide shift reagents have been reported for recognizing optical isomers in solution by NMR,[8,24] only a few of them have used optically active polymers as a chiral selector.[15,25] On the basis of the measurement with enantiomerically pure *(R)*- and *(S)*-**2**, it became clear that the hydroxy protons (*(S)*-**2**-OH) were more largely shifted to downfield accompanying with line broadening than the corresponding *(R)*-**2**-OH, whereas the *(S)*-**2**-H4 and -H6 resonances exhibited upfield shift and broadening, indicating that *(S)*-**2** interacts more strongly with **1**. The downfield shift of the OH resonances is ascribed to hydrogen bond effects,[5a,26] and the upfield shifts for the aromatic protons of **2** are probably due to π-stacked or shielding effect by a neighboring aromatic ring of **1**.[27] The significant broadening of these proton resonances of *(S)*-**2** indicates that exchange rates between the free and bound forms of **2** to **1** is slow compared with the NMR time scale,[25,28] although a clear coalescence point could not be observed from dynamic NMR experiments of the mixture at temperatures from +60 to −40 °C in $CDCl_3$. As the temperature was lowered, the resonances of the *(S)*-OH, -H4 and -H6 protons were more broadened. The larger chemical shift movement and broadening of the *(S)*-**2** resonances than (*R*)-**2** observed in the ^{1}H NMR is associated with the chromatographic elution order of the enantiomer.

Discrimination of enantiomers in ^{1}H NMR was also observed for (*RS*)-**4** in the presence of **1**, and the structural features of binding were similar to that for **1**−(*RS*)-**2** complexation; the OH proton resonances were split into two peaks with large downfield shifts (Δδ = 0.563 and 0.165 ppm for (*S*)- and (*R*)-**4**, respectively). The lower-field, broad peak can be assigned to the (*S*)-OH protons, and these observations are consistent

(24) For reviews, see: (a) Rinaldi, P. L. *Prog. Nucl. Magn. Reson. Spectrosc.* **1982**, *15*, 291−352. (b) Weisman, G. R. In *Asymmetric Synthesis;* Morrison, J. D., Ed.; Academic Press: New York, 1983; Chapter 8. (c) Fraser, R. R. In *Asymmetric Synthesis;* Morrison, J. D., Ed.; Academic Press: New York, 1983; Chapter 9.

(25) DNA as a chiral polymer (^{1}H NMR): (a) Rehmann, J. P.; Barton, J. K. *Biochemistry* **1990**, 29, 1701−1709. Polypeptides as a chiral polymer (^{2}H NMR): (b) Lafontaine, E.; Bayle, J. P; Courtieu, J. *J. Am. Chem. Soc.* **1989**, *111*, 8294−8296. (c) Canet, J.-L.; Fadel, A.; Salaün, J.; Canet-Fresse, I.; Courtieu, J. *Tetrahedron Asymmetry* **1993**, *4*, 31−34. (d) Meddour, A.; Canet, I.; Loewenstein, A.; Péchiné, J. M.; Courtieu, J. *J. Am. Chem. Soc.* **1994**, *116*, 9652−9656. (e) Canet, I.; Courtieu, J. *Tetrahedron Asymmetry* **1995**, *6*, 333−336. Cellulose esters as a chiral polymer (^{13}C NMR): see ref 15a.

(26) (a) Dobashi, Y.; Dobashi, A.; Ochiai, H.; Hara, S. *J. Am. Chem. Soc.* **1990**, *112*, 6121−6123. (b) Nishiyama, H.; Tajima, T.; Takayama, M.; Itoh, K. *Tetrahedron Asymmetry* **1993**, *4*, 1461−1464.

(27) Zimmerman, S. C.; Wu, W.; Zeng, Z. *J. Am. Chem. Soc.* **1991**, *113*, 196−201.

(28) Collins, J. G.; Shields, T. P.; Barton, J. K. *J. Am. Chem. Soc.* **1994**, *116*, 9840−9846.

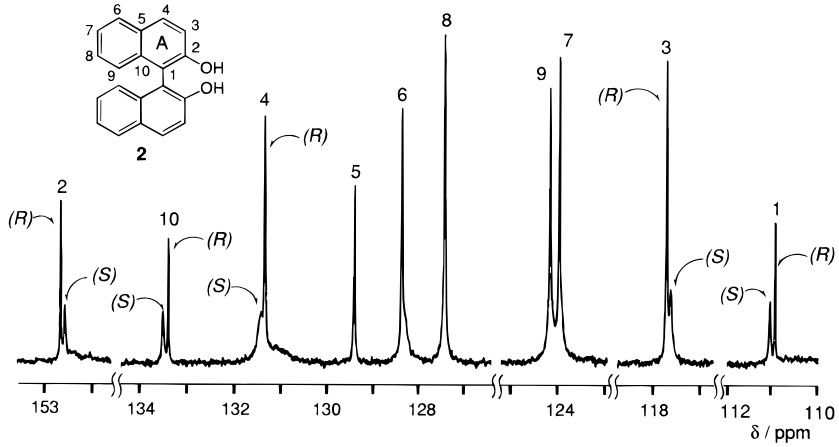

Figure 3. ^{13}C NMR spectrum of (*RS*)-**2** (116 mM) in the presence of **1** (54.2 mM) in $CDCl_3$ at 23 °C.

Table 3. ^{13}C NMR Chemical Shifts (ppm) of **4** in the Absence and the Presence of **1** in $CDCl_3$ at 23 °C

position	free[a]	**1**−(*S*)-**4**[b]	**1**−(*R*)-**4**[b]	$\Delta\Delta\delta$[c]
2	153.81	153.72	153.78	−0.06
3	113.16	113.06	113.12	−0.06
4	130.12	130.06	129.99	0.07
5	122.59	122.58	122.51	0.07
6	138.94	139.07	138.95	0.12

[a] [(*RS*)-**4**] = 156 mM. [b] [(*R*)- or (*S*)-**4**] = 156 mM, [**4**]/[**1**] = 2.88. [c] Obtained by subtracting the **1**−(*R*)-**4** values from the **1**−(*S*)-**4** ones.

with the chromatographic enantioseparation results (Table 1). However, for **3a** and **3b**, no splitting due to the enantiomers was observed in the presence of **1**. These NMR results also support the importance of the hydrogen bonding of the two hydroxy groups for chiral discrimination as seen in the chiral HPLC. The racemate **5** was hardly separated in ^1H NMR as well as in HPLC. These ^1H NMR data are fully consistent with the chromatographic data with respect to the enantioselectivity and elution order.

Similar splittings of **2** and **4** into enantiomers in the presence of **1** were also observed in ^{13}C NMR spectroscopy. Figure 3 shows the 125 MHz ^{13}C NMR spectrum of (*RS*)-**2** in the presence of **1** in $CDCl_3$. The carbon resonances of free **2** were unambiguously assigned from the $^1H-^{13}C$ COSY experiment. In Figure 3, it is apparent that the C1−C4 and C10 resonances are enantiomerically separated and the *(S)*-**2** carbon resonances are markedly broadened as seen in its ^1H NMR spectrum (Figure 2). In Table 2 are summarized the ^1H and ^{13}C NMR chemical shifts of *(R)*- and *(S)*-**2** in the presence and absence of **1**. Chemical shift differences between the corresponding proton or carbon resonances of *(R)*- and *(S)*-**2** were obtained by subtracting the *(R)*-**2** values from the *(S)*-**2** ones. The carbons (C1−C4 and C10) exhibiting large splits ($\Delta\Delta\delta$) belong to ring A (see Figure 3), indicating that ring A may be favorably located close to the chiral glucose residue; in other words, (*S*)-**2** may insert from ring A into the chiral groove of **1** to form the hydrogen bond involving the two hydroxy groups of (*S*)-**2** and the carbamate residues of **1** (see below for detailed discussion).

Some carbons of (*RS*)-**4** were also split into enantiomers in the presence of **1** (Table 3).

Two-Dimensional NMR Studies. The recent development of 2D NMR techniques has provided a powerful tool for constructing the structures of biopolymers and synthetic polymers and for elucidating the interaction occurring in host−guest bimolecular systems such as biopolymers and drugs. In particular, a 2D NOESY spectroscopy is very useful to obtain interproton distances, which provide information on the conformation of polymers and its interaction with another molecule at a molecular level.[16]

In the NOESY spectrum of the free polysaccharide derivative **1**, a number of NOE cross peaks were observed in the region of glucose−glucose, aromatic−aromatic, and aromatic−methyl proton resonances (see the supporting information). The chemical shifts of the glucose protons (H1−H6) of **1** were identical within 0.1 ppm to those of cellulose triacetate (CTA) in $CDCl_3$ reported by Buchanan *et al.*,[29] and the NOE cross peak pattern of the glucose proton resonances was also similar, indicating that the glucose unit of **1** may have a conformation similar to that of CTA. Buchanan *et al.* proposed a 5/4 helical structure for CTA based on the calculated interproton distances of the glucose protons, *e.g.*, H1−H4′ (a prime represents a nuclei of the adjacent glucose residue), by measuring peak volumes of cross and diagonal peaks at a different short mixing times (60−100 ms).[29] They did not provide sufficient data for determining the torsion angle about the glycoside bond defined by two dihedral angles (H1−C1−O−C4′−H4′), although a certain torsion angle was determined using molecular models of CTA postulated by X-ray analysis. We attempted to estimate the peak volumes of cross peaks in the glucose proton resonances of **1** by means of the NOESY method acquired at different short mixing times (60−150 ms) to determine the torsion angle of the glycoside bond of **1** according to the Buchanan's method. Although it was difficult owing to the broadening of the peaks and the overlapping in some glucose protons, we could use the structural data of a cellulose derivative, cellulose tris(phenylcarbamate) (CTPC), to construct a molecular model of a CTPC derivative **1**; the structure of crystalline CTPC was determined to be a left-handed 3/2 helix by X-ray analysis.[30] Analogous cellulose derivatives, cellulose tribenzoate[31] and cellulose tris(4-chlorophenylcarbamate),[32] have been reported to have the same left-handed 3/2 helical structure by means of X-ray analysis. Moreover, it was reported from light scattering and viscometry measurements that CTPC may hold a similar helical structure even in solution.[33,34] On the basis of these reported structure data, we are able to build up a model polymer as described later.

(29) Buchanan, C. M.; Hyatt, J. A.; Lowman, D. W. *J. Am. Chem. Soc.* **1989**, *111*, 7312−7319.

(30) (a) Zugenmaier, P.; Vogt, U. *Makromol. Chem.* **1983**, *184*, 1749−1760. (b) Vogt, U.; Zugenmaier, P. *Ber. Bunsenges. Phys. Chem.* **1985**, *89*, 1217−1224.

(31) Steinmeier, H.; Zugenmaier, P. *Carbohydr. Res.* **1987**, *164*, 97−105.

(32) Riehl, K. Ph.D. Thesis, Technischen Universität Clausthal, Germany, 1992.

(33) Danhelka, J.; Netopilík, M.; Bohdanecky, M. *J. Polym. Sci. Part B: Polym. Phys.* **1987**, *25*, 1801−1815.

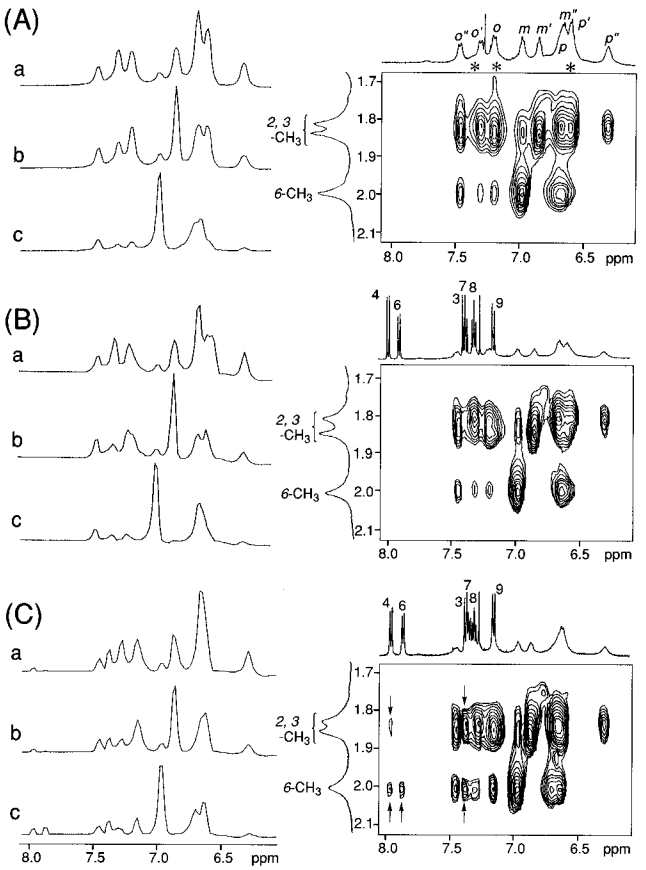

Figure 4. Expanded NOESY spectra (right hand side) at a mixing time of 300 ms of the free **1** (A) and the mixtures of (*R*)-**2** and **1** (B) and (*S*)-**2** and **1** (C) (molar ratio, 1:2) in the region between the aromatic protons (**1** and **2**) and methyl protons on the phenyl moiety of **1** in $CDCl_3$ at 30 °C. The concentration of **2** was 9.7 mM. Asterisks in A indicate the possible chemical shifts of the NH proton resonances of **1**. The aromatic proton resonances of **1** are denoted by *o* (*ortho*), *m* (*meta*), and *p* (*para*). The arrows (C) indicate intermolecular NOE cross peaks observed between the aromatic H4, H6, and H7 protons of *(S)*-**2** and the methyl protons of **1**. On the left hand side are shown the column slices taken through the tops of the three methyl peaks on the phenyl groups introduced at the 2,3- (a and b) or 6-position (c) of a glucose unit of **1**.

Figure 4 shows the NOESY spectra of free **1** (A), **1**−(*R*)-**2** (B), and **1**−(*S*)-**2** (C) (molar ratio, 2:1) in the regions between the aromatic protons (**1** and **2**) and the methyl protons on the phenyl group of **1**. The aromatic proton resonances [*ortho* (*o*), *meta* (*m*), and *para* (*p*)] were assigned from the COSY spectrum, but the 2-, 3-, or 6-position of a glucose unit could not be identified. The assignment of the methyl proton resonances on the phenyl groups introduced at the 2-, 3-, or 6-position of a glucose unit was attained by comparing the NMR data of a regioselectively carbamoylated model polymer, cellulose 6-(5-fluoro-2-methylphenylcarbamate)2,3-bis(4-chlorophenylcarbamate). A similar chemical shift difference of the methyl protons on the phenyl groups depending on the position of a glucose residue has been observed for other methylphenylcarbamates of cellulose.[35] The assignment of the two methyl protons at the 2- and 3-positions has not yet been attained because of the difficulty of regioselective substitution on the two hydroxy groups at the 2- and 3-positions of a glucose.

(34) The monomeric length (*h*) along the contour of the CTPC chain was estimated to be 0.51 nm based on the data taken from ref 33, which is in agreement with the pitch per residue (0.51 nm) of the left-handed 3/2 helix for the crystalline CTPC.[30] A similar observation has recently been reported for cellulose tris(3,5-dimethylphenylcarbamate): Tsuboi, A.; Yamasaki, M.; Norisue, T.; Teramoto, A. *Polym. J.* **1995**, *27*, 1219−1229. However, these agreements do not necessarily indicate that the CTPC and its derivatives maintain the same helical conformation in solution, because the *h* value is close to the monomeric projection for other cellulose derivatives with a different conformation.

Table 4. Spin−Lattice Relaxation Times (T_1/s) of **2** in the Absence and Presence of **1** in $CDCl_3$ at 19 °C[a]

	position	(*R*,*S*)-**2**[b]	**1**−(*S*)-**2**[c]	**1**−(*R*)-**2**[c]
^{13}C	1	11.93	7.47	8.82
	2	7.68	4.20	5.31
	3	1.38	0.90	1.07
	4	1.30	0.82	0.99
	5	6.11	3.07	4.03
	6	1.29	0.97	1.02
	7	1.18	0.90	0.93
	8	1.31	0.86	1.01
	9	1.28	0.92	1.00
	10	6.69	2.98	4.15

[a] The measurements of T_1s were carried out three times, and the deviation was less than 3%. [b] [(*R*,*S*)-**2**] = 116 mM. [c] [(*S*)- or (*R*)-**2**] = 58.2 mM, [**2**]/[**1**] = 1.07.

On the left side of the contour plots in Figure 4 are shown column slices taken through the tops of these three methyl peaks on the phenyl groups of **1**. In the spectrum of free **1** (A), many cross peaks were observed. Most of them can be ascribed to intramolecular NOEs between the methyl and aromatic protons on the same phenyl ring, though some of them cannot. These unassigned NOEs may be due to those between the NH proton and methyl protons or between the aromatic protons and the methyl protons on a different phenyl residue. Three NH proton resonances should exist at around 6.5−7.5 ppm. However, these resonances could not be clearly observed at 30 °C. At 60 °C, one clear and two rather broad NH resonances appeared in this region, and their possible chemical shifts at 30 °C are marked by asterisks in Figure 4A. These NH protons may be positioned closely to the methyl protons showing NOEs.

The 1:2 mixture of *(R)*-**2** and **1** (Figure 4B) exhibited a NOESY spectrum very similar to the spectrum of Figure 4A, and no intermolecular NOE cross peaks between **1** and *(R)*-**2** were observed, indicating that a weak interaction exists between them. This observation is in accord with the results in the chiral HPLC and 1D NMR experiments. On the other hand, some clear intermolecular NOE cross peaks being represented by arrows in Figure 4C were observed between the aromatic H4, H6, and H7 protons of *(S)*-**2** and the methyl protons of **1** under identical conditions. These data indicate that (*S*)-**2** binds or interacts with **1** more strongly than (*R*)-**2**, and the naphthyl protons of (*S*)-**2** are located closely to the methyl protons of **1** within less than 5 Å. All the intra- and intermolecular NOE enhancements were negative as shown in the column slices, which are often seen in 2D NOESY spectra of biopolymer−drug complexes, indicating that the **1**−(*S*)-**2** complex appears to be in the slow motion regime ($\omega_0\tau_0 > 1.1$).[5c,8k,16c] The strongest intermolecular NOE cross peaks observed are between the 6-methyl protons and H4 and H6 of (*S*)-**2** and the 2- or 3-methyl protons and H7 of (*S*)-**2**. These observations may be useful in order to construct a structural model for the complexation between (*S*)-**2** and **1**. In the aromatic−aromatic region of the NOESY spectrum, however, there exist no clear intermolecular cross peaks, even when the NOESY spectra were acquired at different mixing times (60, 80, 150, 300, and 500 ms).

Complexation and Dynamics. An indication of different dynamics of the two enantiomers bound to **1** was obtained through the examination of relaxation properties of the enantiomers in the presence of **1** (Table 4). Spin−lattice relaxation

(35) Kaida, Y.; Okamoto, Y. *Bull. Chem. Soc. Jpn.* **1993**, *66*, 2225−2232.

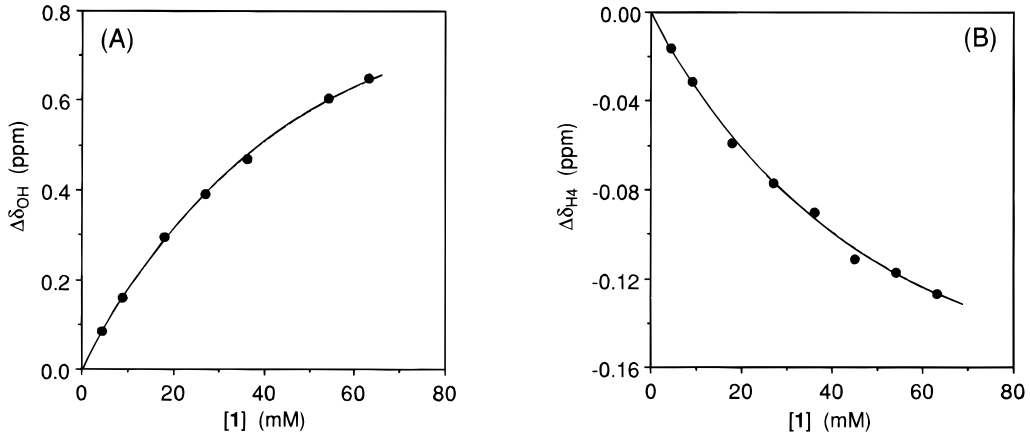

Figure 5. ^{1}H NMR titrations of (*S*)-**2** (1.94 mM) with **1** (0−63.2 mM) in $CDCl_3$ at 23 °C. The changes in chemical shifts of OH (A) and H4 (B) proton resonances of (*S*)-**2** were followed. Negative value indicates an upfield shift.

time (T_1) is sensitive to molecular motions, and therefore, is useful to know how the mobility differs between the enantiomers of **2** in the presence of **1**. All carbons of *(R)*- and *(S)*-**2** in the presence of **1** showed shorter T_1s than those of the free **2**, and those for *(S)*-**2** were always shorter than the corresponding T_1 of the *(R)*-**2**. Remarkable reduction of the T_1 was observed for the C1−C5 and C10 carbons attached to the ring A (see Figure 3). These results indicate that the mobility of the ring A bearing hydroxy groups was unequivocally restricted probably due to binding to the polymer **1** through the intermolecular hydrogen bond between the OHs at the C2 carbons in the ring A and the C═O of carbamate residues of polymer **1**.

Measurements of ^{1}H spin−lattice relaxation time also support the above speculation. In the presence of **1**, the T_1s for the H4 and H6 of (*S*)-**2** were 2.4 and 2.6 s, respectively, whereas those for the (*R*)-**2** were 2.8 and 2.9 s, respectively; those values are shorter than the T_1s of free **2** (2.9 and 3.0 s, respectively).

The standard titration experiments of (*S*)- and (*R*)-**2** in the presence of **1** at various temperatures were carried out by means of ^{1}H NMR spectroscopy in order to estimate the binding constants (K_S and K_R) per glucose unit for (*S*)- and (*R*)-**2** and the thermodynamic parameters $\Delta G°$, $\Delta H°$, and $\Delta S°$ for the complexation; $\Delta G°$ is the change in total free energy, and $\Delta H°$ and $\Delta S°$ represent the association changes in enthalpy and entropy, respectively. The ratio of each binding constant obtained at different temperatures can lead to $\Delta\Delta G°$, $\Delta\Delta H°$, and $\Delta\Delta S°$ values through standard relations (eq 2)

$$\Delta\Delta G° = -RT\ln(K_S/K_R) = \Delta\Delta H° - T\Delta\Delta S° \qquad (2)$$

where the terms $\Delta\Delta G°$, $\Delta\Delta H°$, and $\Delta\Delta S°$ represent the differences in the total free energy, enthalpy, and entropy, respectively.

The ^{1}H NMR titrations were carried out under the conditions of constant [**2**] with varying [**1**] at 23, 30, 40, 50, and 60 °C in $CDCl_3$. Addition of **1** to a solution of (*S*)-**2** caused downfield shifts of the OH resonances, while the aromatic H4 and H6 resonances showed upfield shifts. Downfield shifts are expected for the proton involved in a hydrogen bonding, and upfield shifts are often seen for the aromatic residues which are π-stacked. Figure 5 shows the titration curves between (*S*)-**2** and **1** at 23 °C in $CDCl_3$, where negative values indicate an upfield shift. The titration curves in the figure were analyzed by both linear (eq 3: method A)[36] and nonlinear (eq 4: method B)[37] least-square methods using a binding model with a 1:1 polymer (one glucose unit)−guest stoichiometry and are in agreement with the 1:1 complexation. Because of solubility limit of **1** and **2** in $CDCl_3$, the maximum $[\mathbf{1}]_t/[\mathbf{2}]$ was less than *ca.* 40 (t = total). Thus, the titration data were analyzed using the following two equations to reduce errors and to evaluate correctly the binding constant (K_S)

$$1/\Delta\delta = 1/\Delta\delta_{max} + 1/(\Delta\delta_{max}K_S[\mathbf{1}]_t) \qquad (3)$$

$$[\mathbf{1}]_t/\Delta\delta = ([\mathbf{1}]_t + [\mathbf{2}]_t - [\mathbf{2}]_t\Delta\delta/\Delta\delta_{max})/\Delta\delta_{max} + 1/(\Delta\delta_{max}K_S) \qquad (4)$$

where $\Delta\delta$ and $\Delta\delta_{max}$ are the observed and calculated maximum chemical shift changes, respectively. All data were used for calculating $\Delta\delta_{max}$ and K_S in eq 4, while the concentrations of **1** and **2** were chosen so as to meet the Benesi−Hildebrand conditions (eq 3; $[\mathbf{1}]_t/[\mathbf{2}]_t \geq 10$).[36a] The chemical shift changes in OH and H4 resonances of (*S*)-**2** gave K_S = 15.5 and 15.7 M^{-1}, respectively, for eq 3, which are in reasonably consistent agreement with K_S = 17.1 and 18.0 M^{-1}, respectively, for eq 4. In the former case, plots of $1/\Delta\delta$ versus $1/[\mathbf{1}]_t$ led to a linear relation with a correlation coefficient $r > 0.992$, and the standard deviations of the calculated values from the experimental ones in the curve fitting using eq 4 were below 10%. The K_S and $\Delta\delta_{max}$ values obtained at different temperatures are listed in Table 5.

The 1:1 complexation was also confirmed by the continuous variation plot (Job plot) for the **1**−(*S*)-**2** complex (Figure 6) in which the total concentrations of **1** and (*S*)-**2** were kept constant at 25 mM. The maximal complex formation occurred at around 0.5 mol fraction of **1**. This result implies that each glucose unit of the polymer **1** has the same binding affinity to (*S*)-**2**, which may be attributed to the regular structure of **1** even in a solution. If the polymer had a random coil conformation in solution, there might exist a number of binding sites interacting with a guest in different ways. This would lead to a different complex from the 1:1 complex. The regular structure of **1** must be responsible for the efficient chiral recognition capability in NMR as well as in HPLC.

(36) (a) Kobayashi, K.; Asakawa, Y.; Kato, Y.; Aoyama, Y. *J. Am. Chem. Soc.* **1992**, *114*, 10307−10313. (b) Kelly, T. R.; Kim, M. H. *J. Am. Chem. Soc.* **1994**, *116*, 7072−7080.

(37) (a) Diederich, F. *Angew. Chem., Int. Ed. Engl.* **1988**, 27, 362−386. (b) Takai, Y.; Okumura, Y.; Takahashi, S.; Sawada, M.; Kawamura, M.; Uchiyama, T. *J. Chem. Soc., Chem. Commun.* **1993**, 53−54. (c) Sawada, M.; Okumura, Y.; Shizuma, M.; Takai, Y.; Hidaka, Y.; Yamada, H.; Tanaka, T.; Kaneda, T.; Hirose, K.; Misumi, S.; Takahashi, S. *J. Am. Chem. Soc.* **1993**, *115*, 7381−7388. (d) Albert, J. S.; Goodman, M. S.; Hamilton, A. D. *J. Am. Chem. Soc.* **1995**, *117*, 114−1144. (e) Sawada, M.; Takai, Y.; Yamada, H,; Hirayama, S.; Kaneda, T.; Tanaka, T.; Kamada, K.; Mizooka, T.; Takeuchi, S.; Ueno, K.; Hirose, K.; Tobe, Y.; Naemura, K. *J. Am. Chem. Soc.* **1995**, *117*, 7726−7736.

Table 5. Binding Constants (K_S) for the Complexation of **1** with (*S*)-**2** and Saturation Shifts ($\Delta\delta_{max}$) for the Aromatic H4 and OH of (*S*)-**2**[a]

		method A[b]		method B[c]	
T (°C)		K_S (M^{-1})	$\Delta\delta_{max}$ (ppm)[d]	K_S (M^{-1})	$\Delta\delta_{max}$ (ppm)[d]
23	H4	15.7	−0.257	18.0	−0.241
	OH	15.5	1.32	17.1	1.27
30	H4	15.9	−0.218	17.1	−0.217
	OH	12.4	1.34	14.0	1.27
40	H4	10.1	−0.200	11.4	−0.190
	OH	8.5	1.28	9.5	1.21
50	H4	6.2	−0.196	7.1	−0.180
	OH	4.1	1.66	6.6	1.16
60	H4	4.9	−0.164	5.9	−0.144
	OH	3.0	1.59	4.8	1.09

[a] [(*S*)-**2**] = 1.94 mM and [**1**] = 0−63.2 mM in $CDCl_3$. [b] Estimated by the Benesi−Hildebrand analysis (eq 3 in the text). [c] Estimated by the nonlinear least-squares method (eq 4 in the text). [d] Negative value indicates an upfield shift.

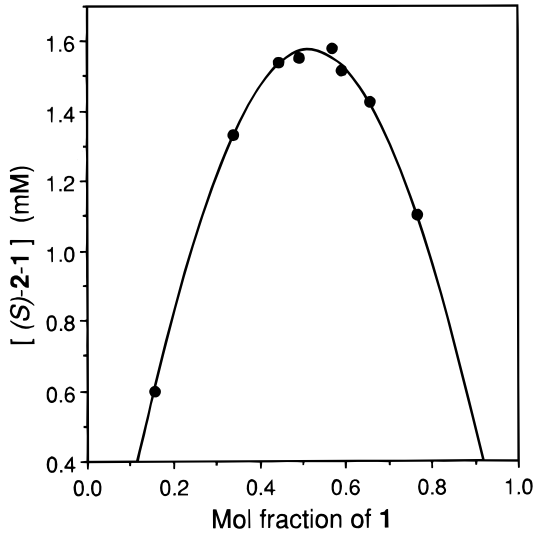

Figure 6. Job plot of (*S*)-**2** with **1** in $CDCl_3$ at 23 °C. The total concentration is 25 mM, and the OH proton resonance of (*S*)-**2** is analyzed.

The titration experiments were carried out for (*R*)-**2** with **1** under the same conditions as above. As expected from the 1D and 2D NMR experiments combined with dynamics data, the binding constant of (*R*)-**2** to **1** was very small (1.5 M^{-1}) at 23 °C. At higher temperatures (≥30 °C) the complexation-induced shifts ($\Delta\delta$) were so small (<0.032 ppm even at $[\mathbf{1}]_t/[(R)\text{-}\mathbf{2}] = 33$) that we could not determine reliable K_R values (≤1 M^{-1}) by ^{1}H NMR titrations. The binding constant K_R at 23 °C was evaluated by the Benesi−Hildebrand analysis for only H4 shifts of the guest (referring to eq 3) because the labile OH proton resonance disappeared after a few hours upon addition of **1** at 23 °C and after a few minutes at higher temperatures (i.e., 50 °C) even with a freshly prepared sample. However, the OH protons of (*S*)-**2** apparently resonated in the presence of **1** even at high $[\mathbf{1}]_t/[\mathbf{2}]$ and at higher temperature ranges (30−60 °C). These results suggest that the OH protons of (*S*)-**2** may not exchange with H_2O in a $CDCl_3$ solution because of tight binding to **1** through hydrogen bonding, while those of (*R*)-**2** exchanged rapidly.[38]

The thermodynamic parameters ($\Delta H°_S$ and $\Delta S°_S$) for the complexation of **1**−(*S*)-**2** in solution were estimated from the linear plot (van't Hoff plot) of ln K_S versus $1/T$ using eq 5.

$$\ln K_S = -\Delta H°/RT + \Delta S°/R \qquad (5)$$

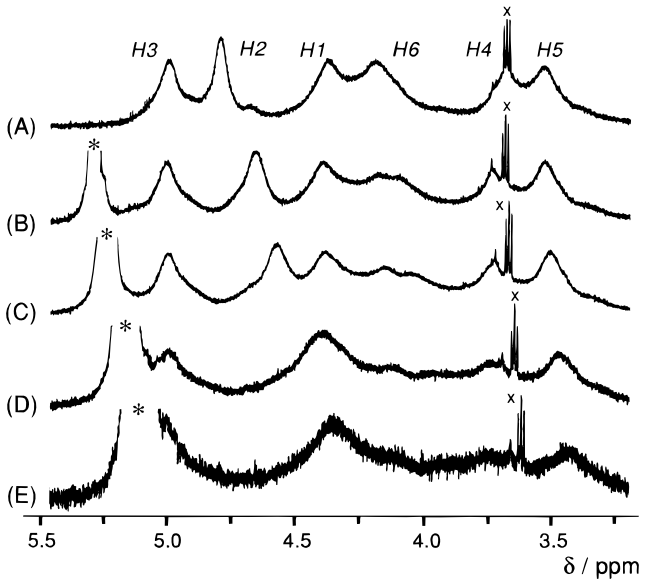

Figure 7. Changes of glucose protons resonances (H1−H6) of **1** (18.0 mM) in the absence (A) and presence of (*S*)-**2** (2.5 (B), 5.0 (C), 15 (D), and 30 mg (E)) in $CDCl_3$ at 23 °C. The marks (× and *) denote the impurity and the OH proton resonances of *(S)*-**2**, respectively.

The plots for the *Ks* values obtained by methods A and B for the OH proton resonances in Table 5 gave $\Delta H°_S = -9.2 \pm 0.8$ and -6.9 ± 0.2 kcal mol^{-1} and $\Delta S°_S = -25.5 \pm 2.6$ and -17.6 ± 0.6 cal mol^{-1} K^{-1}, respectively. The enthalpy factor attributed to hydrogen bonding and π-stacking and/or CH−π interaction overcomes the entropy loss due to the restriction of mobility through hydrogen bonding in the binding process.

Titrations of **1** with (*S*)- and (*R*)-**2** were also performed so as to obtain the information with respect to binding sites of **1** in the complexation. Figure 7 shows the ^{1}H NMR spectra (glucose protons (H1−H6) region) of **1** in the absence and presence of (*S*)-**2**. The H2 proton resonance was dramatically affected by (*S*)-**2** and shifted upfield with binding, while the other glucose proton resonances slightly moved. The significant upfield shifts of the H2 proton resonance indicates that a naphthyl ring of (*S*)-**2** may be closely located above the H2 proton so that it can substantially affect the ring current effect. The chemical shifts changes of **1** against the concentrations of (*S*)- and (*R*)-**2** are plotted (Figure 8). The chemical shift movement of the glucose protons induced by (*R*)-**2** was relatively small.

The ^{19}F NMR chemical shifts of the fluoro groups on the phenyl residues of **1** were analogously altered by the complexation with (*S*)-**2**, while (*R*)-**2** hardly changed the chemical shifts (Figure 9). These different chemical shift changes of **1** against (*S*)- and (*R*)-**2** also support the attractive interaction between (*S*)-**2** and **1**.

Comparison of NMR and HPLC Results. It is particularly interesting to compare the enantioselectivity and thermodynamic parameters measured in solution by the ^{1}H NMR titrations described above with those obtained by chiral HPLC for the binding of **2** with **1**. Recently, it has been reported that in achiral host−guest complexation systems the retention enthalpies ($\Delta H°$) determined by HPLC using a stationary phase consisting of a

(38) We used dry $CDCl_3$ and samples in all NMR measurements, but H_2O bound to the polymer **1** (so called "bound water") could not be removed even after **1** was dried over P_2O_5 in vacuo at 100 °C overnight. The polymer **1** (a repeated glucose unit) was found to contain an almost equimolar amount of bound water from the integral ratio of the ^{1}H NMR spectrum. Direct evidence of the effect of water to binding affinity (*K*) has not yet been obtained. The effects of water on hydrogen bond based molecular recognition of neutral substrates in chloroform, see: Adrian, Jr. J. C.; Wilcox, C. S. *J. Am. Chem. Soc.* **1992**, *114*, 1398−1403.

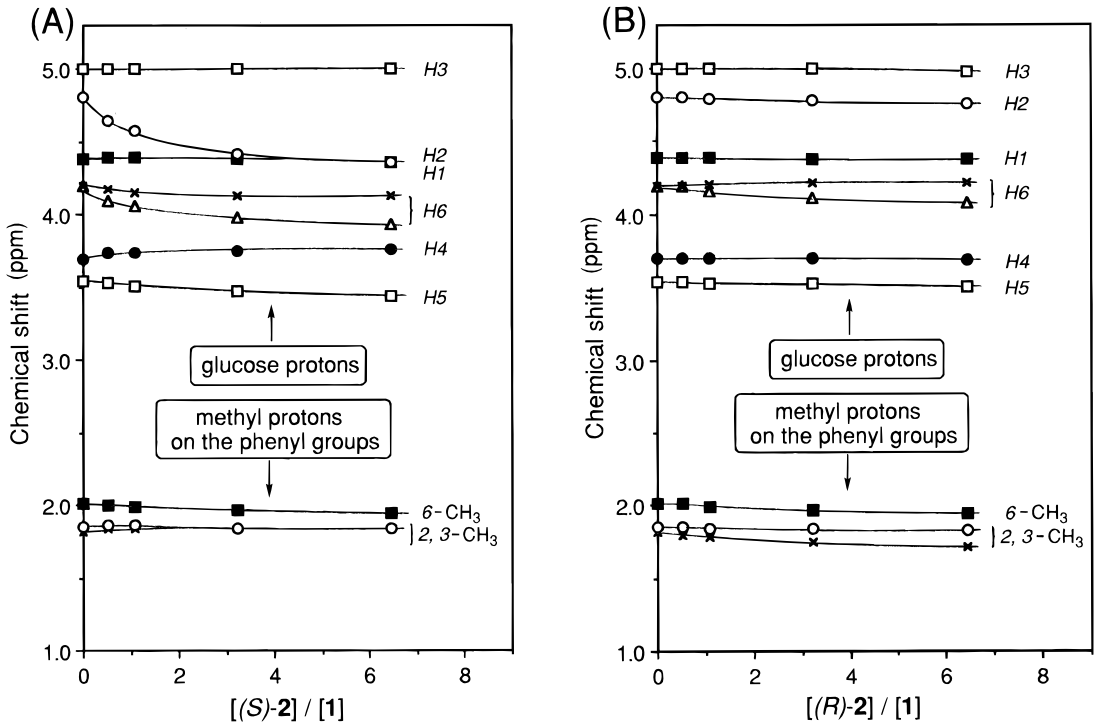

Figure 8. Plots of chemical shifts of glucose protons (H1−H6) and methyl proton resonances of **1** versus [(*S*)-**2**/**1**] (A) and [(*R*)-**2**/**1**] (B) in $CDCl_3$ at 23 °C. The conditions are identical to those shown in Figure 7.

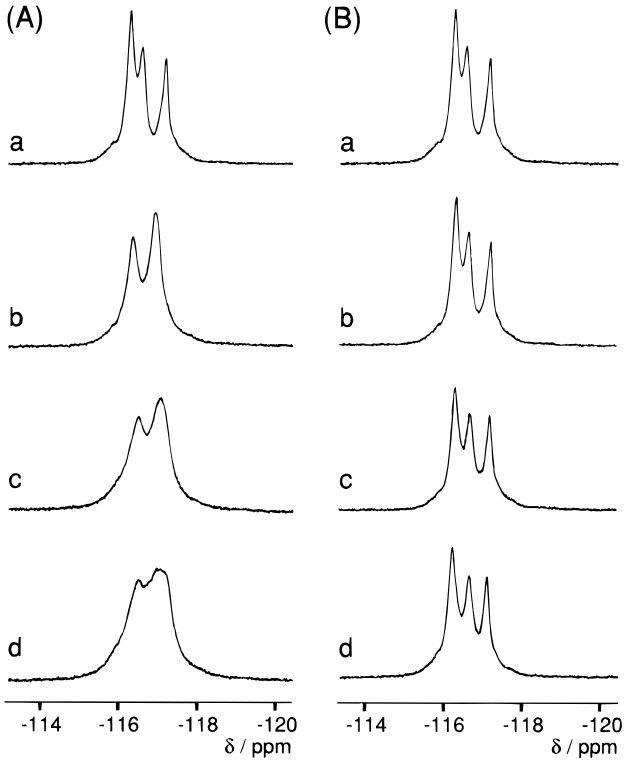

Figure 9. ^{19}F NMR titrations of **1** (18.1 mM) with (*S*)-**2** (A) and (*R*)-**2** (B) (0 (a), 5.0 (b), 15 (c), and 25 mg (d)) in $CDCl_3$ at 23 °C. α,α,α-Trifluorotoluene (−64.0 ppm) was used as the internal standard.

host chemically bonded to silica gel are analogous to the complexation enthalpies measured in solution by ^1H NMR titrations.[39] However, most previous studies concerning the chiral recognition mechanism on chiral stationary phases did not deal with the comparison of $\Delta\Delta G°$ obtained by HPLC and NMR.[40]

From the binding constants, K_S and K_R obtained by the ^1H NMR titrations, the enantioselectivity (α) and the difference in free energy ($\Delta\Delta G°$) upon diastereomeric complexation in solution at 23 °C are calculated to be *ca.* 10.6 and 1.39 kcal mol^{-1}, respectively, using eqs 1 and 2. These values can be compared with those estimated by chiral HPLC; $\alpha = k_2'/k_1' =$ 4.23 and $\Delta\Delta G° = 0.84$ kcal mol^{-1} at 20 °C. The former α value (10.6) is *ca.* 2.5 times larger than that estimated by the chiral HPLC. The difference may be derived from the use of different solvents[5b,i,15b] or unfavorable, nonenantioselective interactions of **2** with the remaining silanol on the surface of silica gel in the chiral HPLC.[41] The chromatographic enantioseparation was carried out using a mixture of hexane-2-propanol, whereas $CDCl_3$ was used for the ^1H NMR experiments. The importance of hydrogen bond association between **1** and **2** for chiral discrimination has been proved by the chiral HPLC and ^1H NMR experiments. Consequently, 2-propanol appears to disturb such an association. Therefore, in the chiral HPLC the separation factor (α) increased as a decrease in the content of 2-propanol in the mobile phase; $\alpha = 3.22$ (mobile phase, 30% 2-propanol in hexane), $\alpha = 4.01$ (20% 2-propanol), and $\alpha = 4.23$ (10% 2-propanol). The influence of 2-propanol on enantioselectivity in solution was also confirmed by the ^1H NMR titrations. When 2-propanol was added to the mixture of **1** and (*RS*)-**2** in $CDCl_3$ under conditions identical to those in Figure 2, $\Delta\Delta\delta$ for the OH and other aromatic proton resonances significantly decreased as an increase in the amount of 2-pro-

(39) Zimmerman, S. C.; Saionz, K. W. *J. Am. Chem. Soc.* **1995**, *117*, 1175−1176.

(40) Pirkle *et al*. have extensively studied chiral recognition in small bimolecular systems relevant to the chiral HPLC by ^1H NMR. They estimated the binding constant (*K*) and thermodynamic parameters ($\Delta G°$, $\Delta H°$, and $\Delta S°$) for the more stable complex by ^1H NMR titrations, although those for the less stable complex could not be determined, probably due to very weak binding.[5c] Very recently, Pinkerton *et al.* compared the $\Delta\Delta G°$ values estimated by chiral HPLC separation of a racemic drug (U-80413) with the third domain turkey ovomucoid chemically bonded silica gel as the CSP and by ^1H NMR titrations of the enantiomers using the protein.[15b]

(41) (a) Pirkle, W. H.; Hyun, M. H. *J. Chromatogr.* **1985**, *328*, 1−9. (b) Dobashi, Y.; Hara, S. *J. Org. Chem.* **1987**, *52*, 2490−2496. Other factors such as loading amount of **1** on silica surface may influence the enantioselectivity.

panol added ($\Delta\Delta\delta_{OH} = 0.021$ and $\Delta\Delta\delta_{H4} = 0.020$ ppm upon addition of 90 μL of 2-propanol).[42] This observation is consistent with the HPLC data. In other words, if the chromatographic experiment is carried out using chloroform as an eluent component, the enantioselectivity may be improved.[43]

Since K_R at higher temperature ranges could not be determined due to very weak binding of (*R*)-**2** with **1** ($K_R < 1\ M^{-1}$), we could not estimate the $\Delta\Delta H°$ and $\Delta\Delta S°$ values by the ^{1}H NMR titrations. However, these parameters can be readily obtained by the chiral HPLC method at a temperature range of $20 \leq T \leq 60$ °C through van't Hoff plots using eq 6[44]

$$\ln \alpha = -\Delta\Delta H°/RT + \Delta\Delta S°/R + \ln(m_{S,T}/m_{R,T}) \qquad (6)$$

where $m_{S,T}$ and $m_{R,T}$ are the binding capacities for *R* and *S* enantiomers at the temperature being examined. If the ratio $m_{S,T}/m_{R,T}$ is constant with temperature, a plot of ln α versus $1/T$ should be linear with a slope of $-\Delta\Delta H°/R$ and an intercept of $\Delta\Delta S°/R$, but if the ratio changes with temperature, the plot of ln α versus $1/T$ should be nonlinear.

The obtained thermodynamic parameters from the linear plots are $\Delta\Delta H° = -2.2 \pm 0.1$ kcal mol^{-1} and $\Delta\Delta S° = -4.9 \pm 0.3$ cal mol^{-1} K^{-1} for **2** and $\Delta\Delta H° = -1.3 \pm 0.1$ kcal mol^{-1} and $\Delta\Delta S° = -2.3 \pm 0.5$ cal mol^{-1} K^{-1} for **4** with hexane−2-propanol (90/10) as the eluent.[45]

Molecular Modeling of the 1−(*S*)-2 Complex. The HPLC and NMR experiments demonstrate that (*S*)-**2** comes in a chiral groove of **1** directed toward the H2 proton of the glucose through intermolecular hydrogen bond between the OH protons and probably the carbonyl oxygens of **1**. Because of the observation of a few intermolecular NOEs for the **1**−(*S*)-**2** complex and the uncertainty of the structure of **1**, a precise model for the complex cannot be drawn. However, a model of the complex can be proposed by using the HPLC and NMR data combined with the structural data of cellulose trisphenylcarbamate (CTPC) determined by X-ray analysis[30] as previously described.

The initial model of **1** was constructed using three-dimensional periodic boundary conditions in CERIUS[2] starting from the CTPC, which is reported to have a left-handed 3-fold (3/2) helical structure, and then was energy-minimized by a Dreiding force field.[46] The initial structure of (*R*)- and (*S*)-**2** was taken from the crystal structure reported for (*RS*)-**2**[47] before minimization (see the Experimental Section). The energy-minimized (*S*)-**2** (Figure 10) was manually placed in the groove of the main chain so that all of the NMR data including the intermolecular NOEs and the titration results as well as intermolecular hydrogen bonds are visually satisfied. The complex was further energy minimized to relieve unfavorable van der Waals contacts. The resulting complex had a negative nonbonded energy, indicating the attractive interaction between **1** and (*S*)-**2** and the absence of any unfavorable contacts.

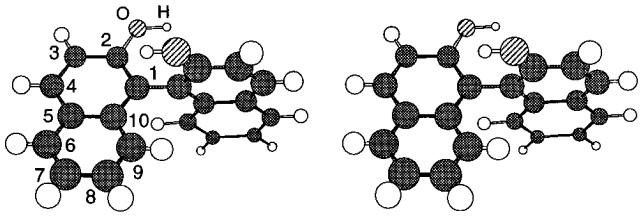

C(2)-C(1)-C(1')-C(2') 97.9°
C(1)-C(2)-O-H -0.7°
C(1')-C(2')-O'-H' -0.8°

Figure 10. Stereoviews of the energy-minimized structure of (*S*)-**2**.

Figure 11 shows the lowest energy structure of the **1**−(*S*)-**2** complex. The polymer possesses a left-handed 3/2 helical conformation, and the glucose residues are regularly arranged along the helical axis. A chiral helical groove, or ditch, with polar carbamate residues exists along the main chain. The polar carbamate groups are located inside, and hydrophobic aromatic groups are placed outside the polymer chain so that polar enantiomers can get in the groove to interact with the carbamate residues *via* hydrogen bonding formation. This interaction seems to be important for efficient chiral discrimination.[14,18]

The location of (*S*)-**2** is best illustrated in Figure 11B, where two OH protons of (*S*)-**2** form hydrogen bonding with the carbonyl oxygens of the carbamate groups at the 2- and 3-positions on two different glucose units (marked by broken line). The distances between the hydrogens and oxygens are 1.97 and 2.24 Å, which are short enough for hydrogen bonding. As shown in Figure 11C, the naphthyl ring protons (H4, H6, and H7) are located close to the methyl protons on the phenyl groups of **1** (CH−π interaction); the distances are 3.51, 4.69, and 3.22 Å, respectively. These results are consistent with the intermolecular NOE data shown in Figure 4. The $\pi-\pi$ interaction between the naphthyl and phenyl rings at the 3-position of a glucose residue may also support the interaction shown in Figure 11C where the distance between the rings is *ca.* 3−3.5 Å. This $\pi-\pi$ interaction appears to contribute to the upfield shifts of H4 and H6 proton resonances of **2**.

The interaction model also explains the upfield shifts of the H2 proton of the glucose residue as illustrated in Figure 11D; the naphthyl ring is favorably positioned above the H2 proton. Moreover, the difficulty of chiral discrimination for 10,10′-dihydroxy-9,9′-biphenanthryl (**5**) is reasonably explained by using the model. Bulky aromatic rings at around the OH groups of **5** may prevent the formation of hydrogen bond.

Although the chromatographic retention behavior for (*R*)-**2** in HPLC and the NMR data, for instance, the downfield shift of the OH proton resonances in the presence of **1**, suggest the existence of weak hydrogen bond interaction between *(R)*-**2** and **1**, it is difficult to propose an analogous model for the **1**−(*R*)-**2** complex because of lack of the NOE data.

When (*R*)-**2** was placed into the groove of **1** in the same way as (*S*)-**2**, the simulation calculation indicated that the (*R*)-**2**

(42) The negative influence of 2-propanol on chiral discrimination in ^{1}H NMR was also observed in a similar $CDCl_3$-soluble CTSP-enantiomer system; the splitting methine proton resonances of *trans*-2,3-diphenyloxirane due to the enantiomers in $CDCl_3$ in the presence of CTSP disappeared by the addition of 15 μL of 2-propanol.[19]

(43) Chloroform cannot be used as the mobile phase on the present chiral stationary phase consisting of **1** coated on silica gel because of solubility problem of **1** in chloroform. The chemically bonded-type CSPs of 3,5-dimethylphenylcarbamates of cellulose and amylose can be used with chloroform as mobile phase component, and a few racemates which were not or poorly resolved on the coated-type CSPs were more efficiently resolved on the chemically bonded-type CSPs with chloroform as a mobile phase component (*i.e.*, hexane−chloroform (95/5)).[14o] The influence of chloroform as a mobile phase component on the chromatographic enantioseparation has also been compared with the ^{1}H NMR data in chiral discrimination using $CDCl_3$ as solvent, see ref 5b,i.

(44) (a) Pirkle, W. H.; Readnour, R. S. *Anal. Chem.* **1991**, *63*, 16−20. (b) Loun, B.; Hage, D. S. *Anal. Chem.* **1994**, *66*, 3814−3822.

(45) When the enantioseparation of **2** and **4** on **1** was performed at high temperatures (30−60 °C), the resolving power of **1** decreased gradually. The α values of **2** and **4** at 20 °C were reduced to 3.81 and 3.00, respectively. However, van't Hoff plots (eq 6) for **2** and **4** gave an almost straight line (see the supporting information).

(46) (a) Mayo, S. L.; Olafson, B. D.; Goddard, W. A., III. *J. Phys. Chem.* **1990**, *94*, 8897−8909. (b) Rappé, A. K.; Goddard, W. A., III. *J. Phys. Chem.* **1991**,*95*, 3358−3363. (c) Castonguay, L. A.; Rappé, A. K.; Casewit, C. J. *J. Am. Chem. Soc.* **1991**, *113*, 7177−7183. (d) Wang, Q.; Stidham, H. *Spectrochim. Acta* **1994**, *50A*, 421−433. (e) Smith, T. L.; Masilamani, D.; Bui, L. K.; Khanna, Y. P.; Bray, R. G.; Hammond, W. B.; Curran, S.; Belles, J. J., Jr.; Binder-Castelli, S. *Macromolecules* **1994**, *27*, 3147−3155.

(47) Mori, K.; Masuda, Y.; Kashino, S. *Acta Crystallogr.* **1993**, *C49*, 1224−1227.

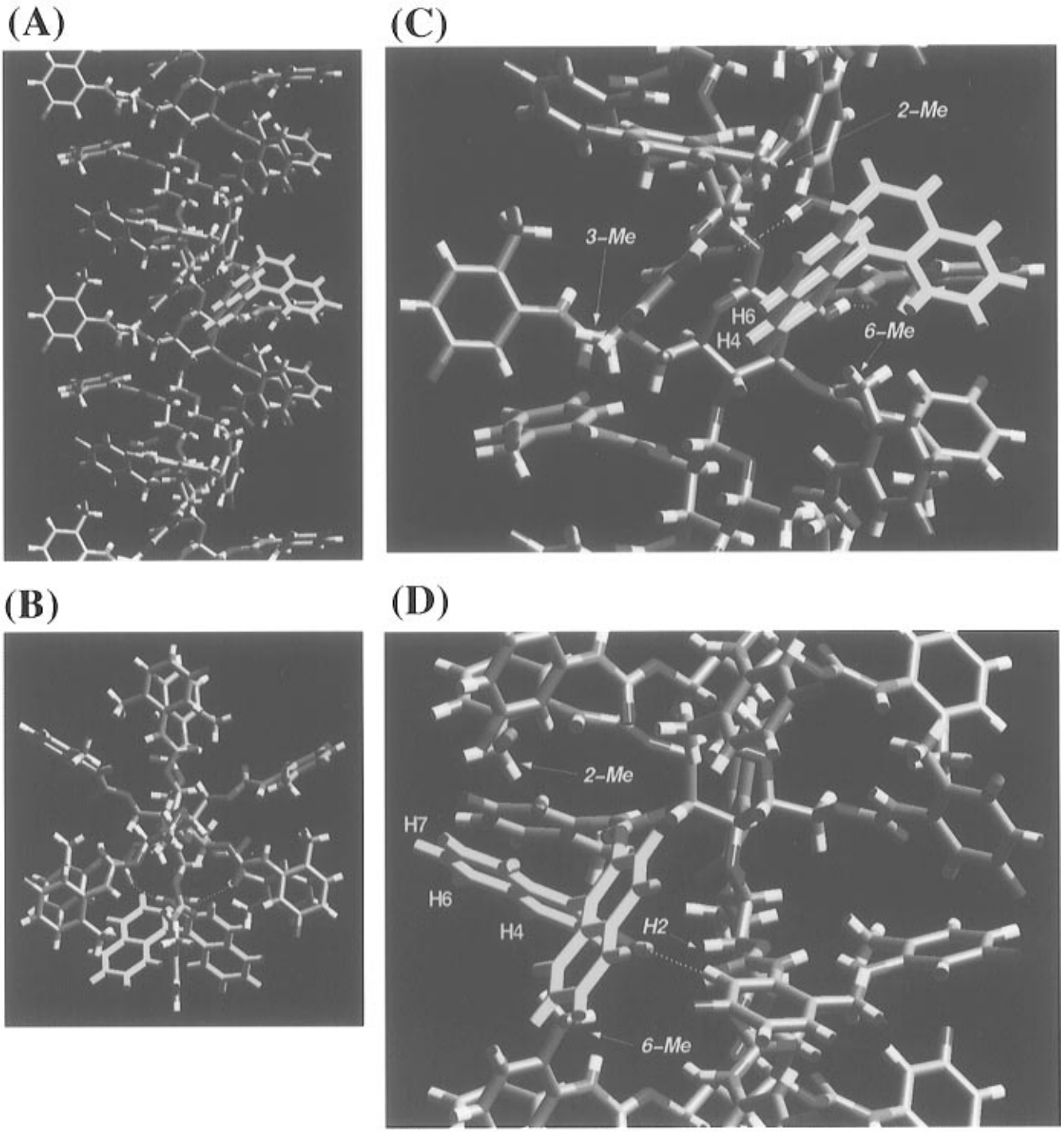

Figure 11. Computer-generated depiction of the complex of **1**−(*S*)-**2**. The (*S*)-**2** is shown in yellow. Dashed lines correspond to hydrogen bonds. (A) Configuration: along the helix axis; (B) perpendicular to the chain axis. (C and D) Expanded region of the same structural model showing the interactions of (*S*)-**2** with **1**.

molecule could not exist in such a way that both the two OH groups can form simultaneous hydrogen bonding to the carbonyl oxygens of the carbamate groups. Only one OH group can form a hydrogen bond. This supports the experimental evidences that (*R*)-**2** forms weaker hydrogen bond with **1** than (*S*)-**2** in the HPLC and NMR experiments.

Conclusions. (*S*)-1,1′-Bi-2-naphthol (**2**) site-selectively binds to the phenylcarbamoylated cellulose derivative **1** through multiple interactions including intermolecular hydrogen bonding and $\pi-\pi$ and/or CH$-\pi$ interactions to afford a 1:1 complex. The molecular modeling on the basis of the chromatography and NMR data reveals the chiral discrimination rationale for a cellulose phenylcarbamate derivative. The enantioselectivities (α) and the thermodynamic parameters $\Delta H°$, $\Delta S°$, and $\Delta G°$ for the more stable complex of **1**−(*S*)-**2** and the difference in free energy ($\Delta\Delta G°$) in chiral discrimination process were separately determined by ^{1}H NMR titrations in solution and by chiral HPLC. These results should provide useful information both for understanding the chiral discrimination mechanism of the other polysaccharide-based CSPs and for designing the more excellent CSPs.

Experimental Section

Materials. Cellulose (Avicel) was purchased from Merck. The degree of polymerization of the cellulose was estimated to be *ca.* 200 as its tribenzoate ester by gel permeation chromatography using THF

as the eluent. 4-Fluoro-2-nitrotoluene, triphosgene, and (3-aminopropyl)triethoxysilane were of guaranteed reagent grade from Tokyo Kasei. Pyridine-d_5 (99 atom % D) was purchased from Aldrich. Porous spherical silica gel (Daiso gel SP-1000) with a mean particle size of 7 μm and a mean pore diameter of 100 nm was kindly supplied by Daiso Chemical. All solvents used in the preparation of CSPs were of analytical reagent grade, carefully dried, and distilled before use. Solvents used in chromatographic experiments were of HPLC grade. $CDCl_3$ (99.8 atom % D, Nacalai) was dried over molecular sieves 4A (Nacalai) and stored under nitrogen.

(±)-1,1′-Bi-2-naphthol (**2**) and *(S)*-(−)-**2** ($[\alpha]^{25}_D$ −32°, *c* 1.5 g dL^{-1}, THF) were purchased from Tokyo Kasei. *(R)*-(+)-**2** ($[\alpha]^{25}_D$ +32°, *c* 1.5 g dL^{-1}, THF) was obtained from Kankyo Kagaku Center. 2-Hydroxy-2′-methoxy-1,1′-binaphthyl (**3a**) and 2,2′-dimethoxy-1,1′-binaphthyl (**3b**) were prepared by alkylation of **2** with methyl iodide in acetone in the presence of K_2CO_3.[48] Racemic and (*R*)-(+)-2,2′-dihydroxy-6,6′-dimethylbiphenyl (**4**) ($[\alpha]^{18}_D$ +91.5°, *c* 1.0 g dL^{-1}, ethanol)[49] were gifts from Dr. Kanoh of Kanazawa University. 10,10′-Dihydroxy-9,9′-biphenanthryl (**5**)[50] was provided by Professor Yamamoto of University of Osaka Prefecture. Ee (>99%) of the enantiomers of **2** and **4** was checked by HPLC using a chiral column consisting of **1** as a CSP. 5-Fluoro-2-methylaniline was prepared by reduction of 4-fluoro-2-nitrotoluene with $SnCl_2 \cdot 2H_2O$ and hydrochloric acid (35%) in ethanol.

Synthesis of Cellulose Tris(5-fluoro-2-methylphenylcarbamate) (1). 5-Fluoro-2-methylaniline (17.0 g, 0.14 mol) was allowed to react with triphosgene (17.8 g, 60 mmol) in dry toluene (380 mL) in the presence of a catalytic amount of dry pyridine (1.0 mL). After evaporation of the solvent, the residue was distilled under reduced pressure (bp 85 °C/28 mmHg) to give 5-fluoro-2-methylphenyl isocyanate (14.4 g, 70%). Cellulose tris(5-fluoro-2-methylphenylcarbamate) (**1**) was prepared according to the previously described procedure[14] by the reaction of cellulose (1.0 g) with a large excess of 5-fluoro-2-methylphenyl isocyanate (6.0 g, 40 mmol) in dry pyridine (20 mL) at *ca.* 80 °C for 40 h.[21] The phenylcarbamoylated cellulose derivative obtained was isolated as a methanol−water (5:1, v/v) insoluble fraction. Elemental analysis and ^{1}H NMR data showed that hydroxy groups of cellulose were almost quantitatively converted into the carbamate moieties. IR (KBr): 3442, 3330 (ν_{NH}), 1742 ($\nu_{C=O}$). ^{1}H NMR (pyridine-d_5, 80 °C, TMS): δ 2.02, 2.04, 2.14 (s, CH_3, 9H), 3.80, 3.97, 4.58, 4.71, 4.85, 5.13, 5.50 (br, glucose protons, 7H), 6.52, 6.68−6.82, 6.91, 6.99, 7.49, 7.67, 7.73 (aromatic, 9H), 8.30, 8.72, 9.24 (br, NH, 3H). $[\alpha]^{25}_D$: −15° (*c* 1.0 g dL^{-1}, THF). Anal. Calcd for $(C_{30}H_{28}O_8N_3F_3)_n$: C, 58.54; H, 4.58; N, 6.83. Found: C, 58.15; H, 4.30; N, 6.90;

Preparation of the Chiral Stationary Phase. A column packing material was prepared as described previously[14] using macroporous silica gel which had been treated with a large excess of (3-aminopropyl)-triethoxysilane in dry benzene in the presence of a catalytic amount of dry pyridine at 80 °C overnight. The cellulose derivative **1** (0.75 g) was dissolved in THF (10 mL), and the silanized silica gel (3.0 g) was wetted with the polymer solution as uniformly as possible. Then, the solvent was evaporated under reduced pressure. The remaining polymer solution was adsorbed on the silica gel using the same procedure. The packing material thus obtained was packed into a stainless-steel tube (25 × 0.46 cm i.d.) by a conventional high-pressure slurry packing technique using a Model CCP-085 Econo packer pump (Chemco). The plate number of the column was 5800 for benzene with hexane−2-propanol (90/10) as the eluent at a flow rate of 0.5 mL min^{-1}. 1,3,5-Tri-*tert*-butylbenzene was used as a nonretained compound for estimating the dead time (t_0).[22]

Instruments. Chromatographic experiments were performed on a JASCO PU-980 chromatograph equipped with a UV (JASCO 875-UV) and a polarimetric (JASCO DIP-181C, Hg without filter) detectors. The column temperature (20, 30, 40, 50, and 60 °C) was controlled with a water jacket. A solution of a racemate or an optically active compound (7.8−14.0 mM) was injected into the chromatographic system (20−100 μL) using a Rheodyne Model 7125 injector with a 1.0 mL loop. One-dimensional ^{1}H, ^{13}C, and ^{19}F NMR spectra and 2-D ^{1}H−^{1}H COSY and NOESY spectra were recorded on a Varian VXR-500S spectrometer operating at 500 MHz for ^{1}H, 125 MHz for ^{13}C, and 470 MHz for ^{19}F. The 2-D ^{1}H−^{13}C COSY spectrum was obtained on a Varian Gemini 200 spectrometer. All NMR spectra were measured in $CDCl_3$ unless specified otherwise. Chemical shifts were reported in parts per million (ppm) with tetramethylsilane (TMS, 0 ppm), $CDCl_3$ (77.0 ppm), and α,α,α-trifluorotoluene (-64.0 ppm) as the internal standard for ^{1}H,^{13}C, and ^{19}F NMR, respectively.

^{1}H NMR Titration. The ^{1}H NMR titration experiments were performed under two conditions. The concentration of **1** was calculated based on glucose units. Condition 1. (*S*)- or (*R*)-**2** was maintained at constant concentration in the presence of increasing concentrations of **1** to measure binding constants (K_S and K_R). Stock solutions (1.94 mM) of (*S*)- and (*R*)-**2** in $CDCl_3$ were prepared. A 0.9 mL aliquot of the stock solution was added using a hypodermic syringe to eight separate vials containing 2.5, 5.0, 10, 15, 20, 25, 30, and 35 mg of **1**, respectively, and the solutions were transferred to eight 5-mm NMR tubes. After the tubes were sealed, ^{1}H NMR spectra were taken for each tube at 23, 30, 40, 50, and 60 °C, and $\Delta\delta$ values were calculated by subtracting the chemical shifts in the spectrum of the mixture from the corresponding resonance of pure **2**. Then, binding constants were determined by using either eqs 3 and 4. Satisfactory fits were observed in all cases for a 1:1 complexation.

Condition 2. The cellulose derivative **1** was maintained at constant concentration in the presence of increasing concentrations of (*S*)- or (*R*)-**2** to obtain information with respect to binding sites of **1** in the complexation. A 18.0 mM solution of **1** in $CDCl_3$ was prepared in a 5-mm NMR tube, and the initial NMR spectrum was recorded. To this was directly added (*S*)- or (*R*)-**2** (2.5, 2.5, 10, and 15 mg, respectively), and NMR spectra were taken for each addition of **2**.

Job Plot. The stoichiometry of the complex between **1** and (*S*)-**2** was determined by the continuous variation plot (Job plot).[51] Stock solutions of **1** and (*S*)-**2** in $CDCl_3$ were prepared (25 mM). In eight NMR tubes, portions of the two solutions were added in such a way that their ratio changed from 0 to 1, keeping the total volume to be 0.8 mL. The ^{1}H NMR spectra for each tube were taken at 23 °C, and the change in chemical shift of the OH proton resonance of (*S*)-**2** was used to calculate the complex concentration using $\Delta\delta_{max} = 1.274$ ppm (see Table 5). The complex concentration was plotted against the mole fraction of **1** to give the Job plot shown in Figure 6.

Spin−Lattice Relaxation Time (T_1). T_1 values were measured without degassing by the inversion-recovery method and calculated by standard programs supplied by Varian. Twelve different τ delays varying from 0.013 to 25.6 s between 180° and 90° pulses with 20 s pulse delay and number of scans of 20 were used for ^{1}H T_1 measurements. T_1s of carbon resonances were measured separately for large ($3 < T_1 < 12$ s) and small ($T_1 \leq 1$ s) values; pulse delay of 55.2 s with eight different τ ($0.625 \leq \tau \leq 80.0$) and 76 scans for the long T_1s, and 6.2 s ($0.125 \leq \tau \leq 8.0$) and 640 times for the short T_1s of free **2**, 36.8 s ($0.275 \leq \tau \leq 35.2$) and 552 times for the long T_1s, and 4.2 s ($0.094 \leq \tau \leq 6.0$) and 3288 times for the short T_1s of *(S)*-(−)-**2** in the presence of **1**, and 47.2 s ($0.375 \leq \tau \leq 48.0$) and 268 times for the long T_1s and 5.2 s ($0.088 \leq \tau \leq 5.6$) and 708 times for the short T_1s of *(R)*-(+)-**2** in the presence of **1**.

2D NMR. NOESY experiments were recorded in the phase-sensitive mode at 30 °C without degassing. The NOESY spectra were collected into 1024 complex points for 256 t_1 increments with spectral widths of 4000 and 5000 Hz for free **1** and (*S*)- or (*R*)-**2** in the presence of **1**, respectively, in both dimensions at mixing times of 60−500 ms. The NOESY spectrum of free **2** was recorded in a similar way with a spectral width of 800 Hz at mixing time of 700 ms. The data matrix was zero filled to 1024 and apodized with a Gaussian function and Fourier transformed in both dimensions. ^{1}H−^{13}C COSY spectrum of free **2** was collected by using a 512 × 128 data matrix size at room temperature. Spectral widths were 2733 and 376.4 Hz for ^{13}C and ^{1}H, respectively.

Molecular Modeling. Molecular modeling and molecular mechanics calculation were performed with the Dreiding force field (version

(48) Galli, B.; Gasparrini, F.; Misiti, D.; Pierini, M.; Villani, C.; Bronzetti, M. *Chirality* **1992**, *4*, 384−388.

(49) Kanoh, S.; Tamura, N.; Motoi, M.; Suda, H. *Bull. Chem. Soc. Jpn.* **1987**, *60*, 2307−2309.

(50) Yamamoto, K.; Fukushima, H.; Okamoto, Y.; Hatada, K.; Nakazaki, M. *J. Chem. Soc., Chem. Commun.* **1984**, 1111−1112.

(51) Job, P. *Ann. Chim. Ser.* **1928**, *9*, 113−134.

2.11)[46] as implemented in CERIUS[2] software (version 1.5, Molecular Simulations Inc., Burlington, MA) running on an Indigo[2]-Extreme graphics workstation (Silicon Graphics). Charges on atoms of **1** and **2** were calculated using Gasteiger in QUANTA (version 4.0, Molecular Simulations Inc.) and QEq[46] in CERIUS[2], respectively; total charges of the molecules were zero. The polymer model of **1** was constructed using the crystalline structure of cellulose trisphenylcarbamate (CTPC)[30] according to the previously reported method with a modification.[18,52] First, a full energy minimization of a repeating unit of **1** containing CH_3O groups at the 1- and 4-positions of a glucose unit was performed by using Conformational Search in CERIUS[2]. The energy minimization was accomplished first by Conjugate Gradient 200 (CG 200) and then by Fletcher Powell (FP) until the root mean square (rms) value became less than 0.01 kcal mol^{-1} $Å^{-1}$, respectively. Next, the monomeric unit of **1** was allowed to construct a trimer with a left-handed 3-fold (3/2) helix by Polymer Builder in CERIUS[2] according to the structure of CTPC.[30] The trimer was placed into a simulation cell ($x = 30$, $y = 30$, and $z = 15.166$ Å) using three-dimensional periodic boundary conditions by Crystal Builder in CERIUS[2]. The unit cell volume was expanded to the directions perpendicular to the polymer axis (z) to avoid interactions of the periodic polymer with neighboring ones in other cells. The energy minimization of the periodic structure was then performed by CG 200 and FP until the rms value became less than 0.01 kcal mol^{-1} $Å^{-1}$, respectively. The resulting optimized trimer in the unit cell was connected to give a nanomer (9mer) as the model polymer of **1** in Figure 11 before placing the (*S*)-**2** or (*R*)-**2** on the interaction site.

The initial coordinates of (*S*)- and (*R*)-**2** were taken from the crystal structure data of (*RS*)-**2**[47] in the Cambridge Structural Database 3D Graphics Search System.[53] The initial structure was further energy-minimized with CG200 and FP using the Dreiding force field. The typical geometric parameters of (*RS*)-**2** before and after minimization are as follows; the torsion angles of C2−C1−C1′−C2′, C1−C2−O1−H, and C1′−C2′−O2′−H for the crystal structure are 88.8, 8.8, and −6.6°, respectively, and 97.9, −0.7, and −0.8° for the optimized structure, respectively (see Figure 10). The optimized (*S*)-**2** was manually placed into the interaction site of **1** so that all of the NMR data including intermolecular NOEs and ^{1}H NMR titration results as well as intermolecular hydrogen bonds were visually satisfied. The complex was further energy minimized by CG200 and FP to relieve unfavorable van der Waals contacts, while the geometry of **1** was fixed. A similar procedure was done for (*R*)-**2**.

(52) Yashima, E.; Noguchi, J.; Okamoto, Y. *Macromolecules* **1995**, *28*, 8368−8374.

(53) Allen, F. H.; Kennard, O. *Chem. Des. Autom. News* **1993**, *8*, 31−37.

Acknowledgment. We thank Professor P. Zugenmaier (Technischen Universität Clausthal) for sending us a copy of Riehl's Ph.D. Thesis. We acknowledge Professor M. Sawada and Dr. Y. Takai (Osaka University) for their kind cession of their fitting programs for ^{1}H NMR titrations. We are also grateful to Professor T. Norisue and Dr. T. Sato (Osaka University) for sending us a copy of their manuscript prior publication and for fruitful discussion. In addition, we thank Professor K. Yamamoto (University of Osaka Prefecture) and Dr. S. Kanoh (Kanazawa University) for providing **5** and **4**, respectively. This work was partially supported by Grant-in-Aids for Scientific Research on Priority Areas No. 06242101 from the Ministry of Education, Science and Culture, Japan.

Supporting Information Available: Copies of 2D NOESY spectra of **1**, **1**−(*S*)-**2**, and **1**−(*R*)-**2**, and van't Hoff plots in the enantioseparation of **2** and **4** at various temperature ranges (4 pages). This material is contained in many libraries on microfiche, immediately follows this article in the microfilm version of the journal, can be ordered from the ACS, and can be downloaded from the Internet; see any current masthead page for ordering information and Internet access instructions.

JA960050X